UNIVERSITY OF CAPE TOWN
IYUNIVESITHI YASEKAPA • UNIVERSITEIT VAN KAAPSTAD

UNIVERSITY OF CAPE TOWN

HONOURS THESIS

Option Valuation and Risk Management under Lévy Jump-Diffusion Models

Authors:
Julian ALBERT
Takudzwa MTOMBENI

Supervisor:
Dr. Etienne PIENAAR

A thesis submitted in partial fulfilment of the requirements for the degree of Bachelor of Commerce (Hons)

in the

Department of Statistics

October 26, 2018

Declaration of Authorship

We, Julian ALBERT & Takudzwa MTOMBENI, declare that this thesis titled, "Option Valuation and Risk Management under Lévy Jump-Diffusion Models" and the work presented in it are our own and confirm that:

- This work was done wholly or mainly while in candidature for the research component of a degree at this University.
- Where any part of this thesis has previously been submitted for a degree or any other qualification at this University or any other institution, this has been clearly stated.
- Where we have consulted the published work of others, this is always clearly attributed.
- Where we have quoted from the work of others, the source is always given. With the exception of such quotations, this thesis is entirely my own work.
- We have acknowledged all main sources of help.
- Where the thesis is based on work done by ourselves jointly with others, we have made clear exactly what was done by others and what we have contributed ourselves.

Signed: _____

Date: _____

Signed: _____

Date: _____

"Nature has established patterns originating in the return of events, but only for the most part. New illnesses flood the human race, so that no matter how many experiments you have done on corpses, you have not thereby imposed a limit on the nature of events so that in the future they could not vary."

Gottfried Wilhelm Leibniz

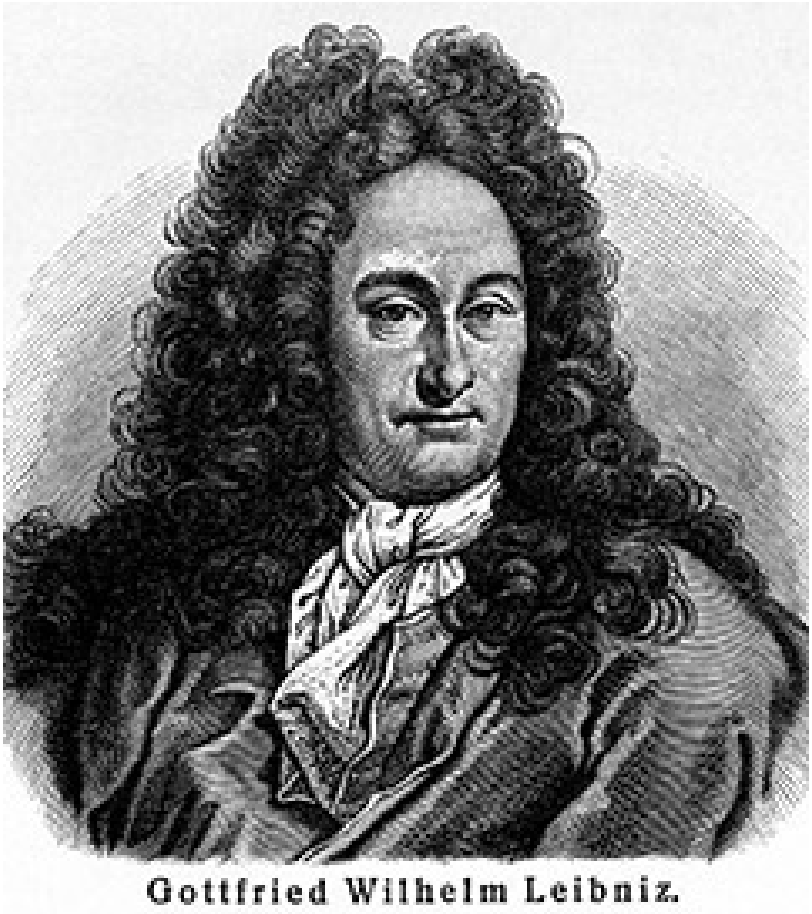

UNIVERSITY OF CAPE TOWN

Abstract

Faculty of Commerce
Department of Statistics

Bachelor of Commerce (Hons)

Option Valuation and Risk Management under Lévy Jump-Diffusion Models

by Julian ALBERT & Takudzwa MTOMBENI

In 1973 Fisher Black and Myron Scholes published their paper "The Pricing of Options and Corporate Liabilities". In it they present a formula for the pricing of options under a geometric Brownian motion model for the prices of the underlying assets [2]. This model is equivalent to assuming that the log returns of shares are normally distributed and share prices evolve continuously.

We show that these simplifying assumptions can lead to severe misestimation of risks in the risk management application. We present a class of models that relax these assumptions in order to better capture market phenomenon and a general framework for how they can be applied in both asset pricing and risk management. We find that when pricing vanilla style options under this class of models we obtain more accurate prices than is achieved under the Black-Scholes framework. In the risk management application we find that this relaxation leads to better fits of the return distributions and significantly different Value-at-Risk estimates.

Acknowledgements

We would first and foremost like to thank our thesis supervisor Dr. Etienne Pienaar from the Department of Statistical Sciences at the University of Cape Town. The door to his office was always open whenever we ran into difficulties or had a question about the research or writing. He consistently allowed us a great deal of freedom in our approach to this topic whilst ensuring we never lost sight of our objectives.

We would also like to thank Mr. Melusi Mavuso and Assoc. Prof. Tim Gebbie for their input. Finally, we express our profound gratitude to our parents and friends for providing us with unfailing support and continuous encouragement throughout our years of study and through the process of researching and writing this research project. This accomplishment would not have been possible without them.

Thank You

Julian ALBERT & Takudzwa MTOMBENI

[0] All share and option price data in this project was sourced from yahoo finance.

Contents

List of Tables

List of Abbreviations

a.s	**a**lmost **s**urely
BAC	Ticker for Bank of America
CDF	**C**umulative **D**istribution **F**unction
CF	**C**haracteristic **F**unction
ECF	**E**mpirical **C**haracteristic **F**unction
EMM	**E**quivalent **M**artingale **M**easure
FFT	**F**ast **F**ourier **T**ransform
L-BFGS	**L**imited Memory **B**royden **F**letcher **G**oldfarb **S**hano
GBM	**G**eometric **B**rownian **M**otion
GMM	**G**eneralized **M**ethods of **M**oments
GS	Ticker for Goldman Sachs.
iff.	**i**f and only **i**f
iid	**i**ndependent and **i**dentically **d**istributed
MLE	**M**aximum **L**ikelihood **E**stimation
MSE	**M**ean **S**quare **E**rror
NYA	Ticker for New York Composite Index
NYSE	**N**ew **Y**ork **S**tock **E**xchange
PDF	**P**robability **D**ensity **F**unction
TSLA	Ticker for Tesla
VaR	**V**alue **a**t **R**isk
WFC	Ticker for Wells Fargo

Chapter 1

Introduction to Option Pricing, the Black-Scholes Framework

1.1 Introduction

An option is a contract associated with an asset, termed the underlying, that entitles the holder the right to purchase or sell the asset at a specified future date[1] and price[2] . The option contract has become very sought after as a means of risk management as investors can combine the various types of options (calls and puts) with positions (long and short) to capture a diverse set of market views. This advantage along with the arguments for option trading being less exposed to the risks associated with trading the underlying asset is what led to the increase in demand for options and with it the need for accurate pricing models. Over the years many of these models have been developed in an attempt to capture the correct value of option contracts, most notably the Black-Scholes formula [2]. Traditional theory utilizes models that lead to closed-form solutions for the option price but make assumptions that do not hold in reality. From a risk management perspective the assumption of normally distributed log returns can lead to severe misestimation of the tail risk associated with a portfolio.

Much of the research towards option pricing and modifying Black-Scholes is aimed at incorporating two empirical features of financial markets; the leptokurtic feature characterised by the distribution of returns exhibiting higher levels of kurtosis with fatter tails, and the volatility smile which describes a phenomenon that is observed when plotting the implied volatility as a function of the strike price where the result often resembles a convex "smiling" curve as opposed to the straight line predicted by the Black-Scholes model. Jump-diffusion models have become an integral part of attempting to solve the problem as the leptokurtic features observed in real data can be partially explained by allowing for jumps in the model. In this paper we present a class of models that relax the geometric Brownian motion assumption of continuous share price sample paths and a general framework for their practical application in both asset pricing and risk management.

This thesis is structured as follows, we proceed with Chapter 1 which introduces the idea of financial market modelling by utilising geometric Brownian motion followed by an introduction to the Black-Scholes framework for option pricing. In Chapter 2 we define Lévy jump-diffusions and outline some of their important properties, we also provide methods for the estimation of their parameters. In Chapter 3 we price options numerically under Lévy jump-diffusions using the Fourier Cosine transform method and compare it's performance to that of the popular Carr-Madan Fourier inversion technique. We then compare

[1] This is referred to as the maturity time of the option.
[2] This is referred to as the strike price of the option.

the prices produced by the Lévy jump-diffusion models to those produced by the Black-Scholes formula. In Chapter 4 we attempt to derive VaR estimates for portfolios comprised of both shares and options where the share prices are modelled using exponential Lévy models, followed by conclusions in Chapter 5.

1.2 Preliminaries

1.2.1 Brownian Motion

Definition A *scalar standard Brownian motion* over $[0, T]$ is a random variable W_t that depends continuously on $t \in [0, T]$ and satisfies the following three conditions [10]:

1. $W_0 = 0$ a.s,
2. For $0 \leq s < t \leq T$ the random variable given by the increment $W_t - W_s$ is normally distributed with mean zero and variance $(t - s)$; equivalently $W_t - W_s \sim \sqrt{t-s}N(0,1)$ where $N(0,1)$ denotes a normally distributed random variable with zero mean and unit variance,
3. For $0 \leq s < t < u < v \leq T$ the increments $W_t - W_s$ and $W_v - W_u$ are independent.

1.2.2 Geometric Brownian Motion

Definition: A process takes on geometric (also known as exponential) Brownian motion (GBM) if its logarithm follows a Brownian motion such that only fractional changes take place as random variation. Otherwise put, a stochastic process S_t (representing asset prices) is said to follow GBM if it satisfies the following differential equation,

$$dS_t = \mu S_t dt + \sigma S_t dW_t. \tag{1.1}$$

Where μ and σ represent the drift and volatility whilst W_t is a standard Brownian motion. In applications to finance we prefer geometric Brownian motion as a simple model for market prices as it takes on non-negative values.

1.2.3 Option Pricing under the Black-Scholes Framework

The success of the Black-Scholes model Equation 1.2 makes it a suitable starting point for any further developments in option valuation. The model assumes that the underlying price follows a geometric Brownian motion, with constant drift and variance, implying that the price of the underlying asset at maturity (S_T) is log-normally distributed.

$$\frac{dS_t}{S_t} = \mu dt + \sigma dW_t \tag{1.2}$$

Assumptions such as continuous sample paths and stationary and independent increments have led the model to not capture some of the stylised facts of real-world stock prices. Figure 1.1 illustrates the leptokurtic feature problem. We interpret that a higher kurtosis suggests that more of the variance is as a result of infrequent extreme deviations, rather than frequent modestly sized deviations. In layman's terms kurtosis quantifies the tail behaviour associated with a distribution. It is clear that by utilising the normal distribution we would underestimate the risk associated with the heavy tails as the empirical return data exhibits a higher level of kurtosis than that of normal distribution.

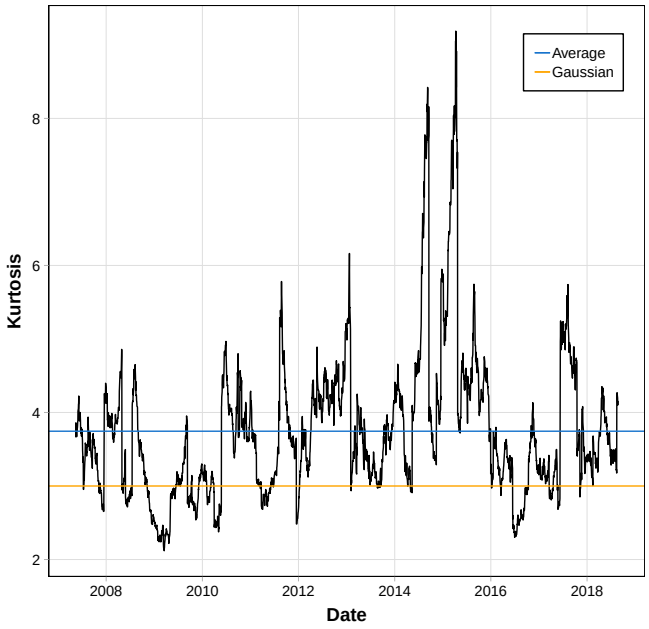

FIGURE 1.1: Kurtosis for a 90 Day Window Rolled over Daily for Naspers Limited (NPN.JO)

1.2.4 Option Pricing under Merton and Kou

Unlike Black-Scholes, models based on Lévy jump-diffusions allow us to incorporate the jumps that occur in real world stock prices. Two of the more notable models that attempt to capture the fat tails are described below. [9] Proposes an extension to the Black-Scholes formulation. He argues that continuous trading (as assumed by [2]) is not possible, thus the validity of their formula depends on the property that for a short time interval the stock price can only deviate in small amounts. The Merton model goes on to decompose the change in stock price into (1) the "normal" price change and (2) the "abnormal" vibration. Where the former is given by a standard geometric Brownian motion with constant variance per unit and the latter - representing new information about the stock that marginally influences the price - being modelled by a "jump" process. We can determine that under these modifications Equation 1.2 is manipulated to look like Equation 1.3 below;

$$\frac{dS_t}{S_t} = \mu dt + \sigma dW_t + \omega dN_t. \tag{1.3}$$

The new term, ωdN_t now represents the "jump" process and can follow any distribution, thus allowing financial models to incorporate distributions with favourable characteristics. In [9] we see the jumps are normally distributed with density

$$\omega = \frac{1}{\sqrt{2\pi\sigma^2}} \exp\left(- \frac{(x-\mu)^2}{2\sigma^2} \right), \tag{1.4}$$

this extension by Merton is important as the introduction of the jump process attempts to capture some of the leptokurtic feature. Merton's jump-diffusion model allows for larger moves in asset prices caused by extreme events as the jump component represents non-systematic risk. The critique of [9] is that the normal distribution used in the stochastic differential equation for the movement of the underlying asset returns is not leptokurtic enough to resemble what is seen in financial market data. [8] Offers explanation for both

the leptokurtosis and the volatility smile critiques by proposing a jump-diffusion model different to that of [9]. Kou's model lets the asset price follow a geometric Brownian motion plus a compound Poisson process with jump sizes double exponentially distributed given by density:

$$\omega = p\eta_1 e^{-\eta_1 y} 1_{\{y \geq 0\}} + p\eta_2 e^{-\eta_2 y} 1_{\{y<0\}}. \tag{1.5}$$

The difference here is that the double exponential (Laplace) distribution when compared to the normal distribution with identical mean and variance, displays a higher peak around the mean, and two heavier tails [8] as illustrated by Figure 1.2. This adjustment is what leads Kou's model for option pricing to (in theory) better account for the leptokurtic feature. Another important property unique to the Laplace distribution is that of the memoryless property, a property responsible for various closed-from solutions [8].

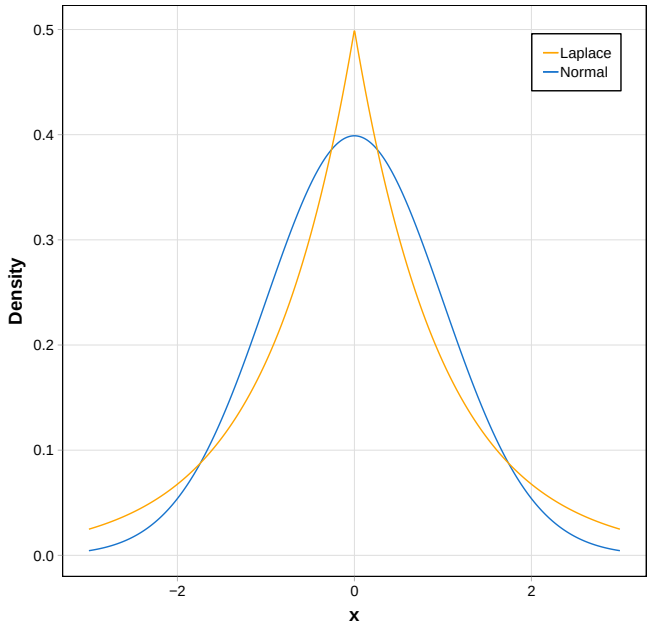

FIGURE 1.2: Double Exponential and Gaussian Distribution with $\mu = 0$ and $\sigma = 1$

Chapter 2

Modelling Share Prices with Lévy Processes

2.1 Lévy Jump-Diffusions

2.1.1 Motivation

Our objective is to generalize the Black-Scholes option pricing framework in order to address the facts that real world share prices do not evolve continuously and that the distributions of the log returns of real shares display significantly fatter tails than can be appropriately modelled by the normal distribution as implied by the Black-Scholes framework. The class of stochastic processes known as Lévy jump-diffusions are a natural initial choice to begin our generalization as this class of processes allows us to fit any infinitely divisible distribution to the log returns thereby allowing us to introduce distributions with heavier tails to model the log returns. Like Brownian motion, Lévy jump-diffusions still have stationary and independent increments which makes simulating the processes conceptually and computationally simple.

2.1.2 Definitions and Relevant Theorems

Definition of a Lévy Process

Let $(\Omega, \mathcal{F}, \mathbb{F}, \mathbb{P})$ be a filtered probability space, an adapted, real valued stochastic process $X = \{X_t\}_{t=0}^{T}$ is a Lévy process if it satisfies the following conditions [6]:

L_1 X is càdlàg,

L_2 $X_0 = 0$,

L_3 X has independent increments,

L_4 X has stationary increments,

L_5 X is stochastically continuous i.e.
$\forall \quad 0 \leq s \leq t \leq T \quad \exists \quad \epsilon > 0 \quad s.t \quad \lim_{s \to t} \mathbb{P}(|X_t - X_s| > \epsilon) = 0.$

From this definition we note that the Brownian motion process used in the Black-Scholes framework is a Lévy process.

The Lévy–Itô Decomposition

Theorem 2.1.1 *Consider a triplet (b, c, v) where $b \in \mathbb{R}$, $c \in \mathbb{R}_{\geq 0}$ and v is a measure satisfying $v(0) = 0$ and $\int_{\mathbb{R}} 1 \wedge |x^2| v(dx) < \infty$. There exists a probability space $(\Omega, \mathcal{F}, \mathbb{P})$ on which four independent Lévy processes exist. $L^{(1)}, L^{(2)}, L^{(3)}$ and $L^{(4)}$, where $L^{(1)}$ is a constant drift, $L^{(2)}$ is a*

Brownian motion, $L^{(3)}$ is a compound Poisson process and $L^{(4)}$ is a square integrable (pure jump martingale) with an a.s. countable number of jumps of magnitude less than 1 on each finite time interval. Taking $L = L^{(1)} + L^{(2)} + L^{(3)} + L^{(4)}$, we have that there exists a probability space on which a Lévy process $L = \{L_t\}_{t=0}^{T}$ is defined. [10]. For the proof of this theorem see [13].

This theorem allows us to decompose any Lévy process into four independent processes. For the sake of this thesis we will only use the subclass of Lévy processes for which the pure jump martingale is zero (i.e. $L^{(4)} \equiv 0$), and we will refer to this subclass of Lévy processes as Lévy jump-diffusions. By the Lévy–Itô decomposition all processes in this subclass can be written as

$$L_t = bt + cB_t + \sum_{i=k}^{N_t} J_k, \tag{2.1}$$

where B_t is standard Brownian motion,
N_t is a poisson process with rate λ,
J_k is a sequence of iid. random variables.

The triplet (b, c, v) is called a Lévy triplet with Lévy measure v. In the case of Lévy jump-diffusions the Lévy measure becomes $v = \lambda \times f$ where f is the law of the iid. random variables J_k. The Lévy triplet $(b, c, \lambda f)$ thus completely characterizes a Lévy jump-diffusion.

The Lévy-Khintchine Formula

The Lévy-Khintchine formula arises as a by product of the Lévy–Itô decomposition and it gives the characteristic function (CF) for any given Lévy process.

Theorem 2.1.2 *If L_t is a Lévy process then its characteristic function is given by:*

$$\mathbb{E}[e^{iuL_t}] = exp\left\{t\big(i\gamma u - \frac{\sigma^2 u^2}{2} + \int_{\mathbb{R}} (e^{iux} - 1 - iux1_{|x|\leq 1})v(dx)\big)\right\}, \tag{2.2}$$

where $L_t = \gamma t + \sigma B_t + Z_t$,
Z_t is a jump process with possibly infintely many jumps.

Applying this formula to the Lévy jump-diffusions, whose jump process has finite jumps, yields a simplified expression for the characteristic function.

Suppose L_t is of the form 2.1. Then its characteristic function is given by:

$$\mathbb{E}[e^{iuL_t}] = exp\left\{t\big(i\gamma u - \frac{\sigma^2 u^2}{2} + \lambda \int_{\mathbb{R}} (e^{iux} - 1)f(dx)\big)\right\}, \tag{2.3}$$

where the jump sizes J_k are distributed according to f.

Theorem 2.1.3 *For every Lévy process $L = (L_t)_{0\leq t\leq T}$ we have that*

$$\begin{aligned}\mathbb{E}[e^{t\psi(u)}] &= e^{t\psi(u)}, \\ &= \exp\left[t\big(ibu - \frac{u^2 c}{2} + \int_{\mathbb{R}} (e^{iux} - 1 - iux1_{\{|x|<1\}})v(dx)\big)\right].\end{aligned} \tag{2.4}$$

Where $\psi(u)$ is the characteristic exponent of L_1, a random variable with an infinitely divisible distribution.

This theorem tells us that the increments of a Lévy process follow the same infinitely divisible distribution, giving us an alternative way of constructing Lévy processes, by specifying a known infinitely divisible distribution on the increments.

2.1.3 Exponential Lévy Models

To ensure non-negativity, stock prices are usually modelled as exponentials of Lévy processes, given by [15];

$$S_t = S_0 e^{X_t}, \tag{2.5}$$

where $X_t = \mu t + \sigma B t + \sum_{i=1}^{N_t} Y_i$. We will refer to X_t as the driving process of the exponential Lévy model. We can see that between the jumps, the process evolves like a geometric Brownian motion, and after the i^{th} jump, the value of S_t is multiplied by $\exp\{Y_i\}$. We stipulate that under the risk-neutral measure the price process discounted at interest rate r, denoted $\{e^{-rt}S_t\}$, must be a martingale and from the Lévy-Khintchine formula 2.2 combined with the independent increments property we conclude that this is the case iff. [15]

$$\mu + \frac{\sigma^2}{2} + \int_{\mathbb{R}} (e^y - 1)v(dy) = 0, \tag{2.6}$$

where the above satisfies no arbitrage opportunity if there exists an equivalent probability $\mathbb{P}^*$ under which $\{e^{-rt}S_t\}$ is a martingale. Thus an exponential Lévy model is arbitrage-free iff. The trajectories of X_t are neither almost surely increasing nor almost surely decreasing [15]. Modelling with respect to the measure $\mathbb{P}^*$ will be further detailed in Chapter 3.

2.2 Simulation of Lévy Models

2.2.1 Simulation via Specification of Jump Distribution

The Lévy–Itô decomposition 2.1, tells us that every Lévy jump-diffusion is comprised of three independent processes. We specify a distribution for the jumps, then simulate the three components of the the Lévy jump-diffusion separately. We then sum the components to create the desired Lévy process. Suppose we wish to simulate a Lévy jump-diffusion specified by the Lévy triplet $(b, c, \lambda f)$ from $t = 0$ to $t = T$ with time steps Δt.

To simulate the Brownian motion component $(bt + cB_t)$, we use the fact that this component has independent and stationary increments and that $(bt + cB_t) \sim N(bt, c^2 t)$. We simulate the increments, $\Delta t \times T$ random variables from $N(bt, c^2 t)$ and take the cumulative sum to obtain $\{bt + cB_t\}_{t=0}^{T}$.

Simulation of the compound Poisson component relies on the following theorem:

Theorem 2.2.1 *Let $T_1, T_2, \cdots, T_n$ be the jump times of a Poisson process N_T, then the distribution of $T_1, T_2, \cdots, T_n | N_T = n$ is the same as that of n independent ordered uniform random variables on $[0, T]$*

Using this theorem and the stationary, independent increment properties of Lévy processes in combination with the fact that all three components of a Lévy jump-diffusion are independent we produce Algorithm 1 for simulating a Lévy jump-diffusion. Suppose this

process is specified by Lévy triplet $(\mu, \sigma^2, \lambda F(x;\boldsymbol{\theta}))$ over the time period $[0, T]$ where $\boldsymbol{\theta}$ is the parameter vector of the jump process and the process is observed every Δt time units.

Algorithm 1 Simulating a Lévy Jump-Diffusion

Generate $T/\Delta t$ random variables $L_i \sim N(\mu, \sigma^2)$
if jump rate = 0 **then**
    return The cumulative sum of (0, $\boldsymbol{L}$)
else
    Generate a random variable $N_T \sim \text{Poisson}(\lambda T)$
    Draw an ordered sample $\boldsymbol{U}$ of size N_t from $u_i \sim U[0, T]$
    Generate N_T random variables $\boldsymbol{Y}$ from $F(x;\boldsymbol{\theta})$
    for t from 1, to T, by step Δt **do**
        $X_t = \text{sum}(\{Y_i : U_i \leq t\})$
    end for

end if
return The cumulative sum of (0, $\boldsymbol{L} + \boldsymbol{X}$)

2.2.2 Simulation via Specification of Infinitely Divisible Distribution

By Theorem 2.1.3 we can use Algorithm 2 to simulate sample paths from a Lévy process with a known increment distribution. Although it is very simple to construct Lévy processes and estimate the parameters of such a processes in this manner, the downside is that we are restricted to the Lévy processes whose increment distribution is known.

Suppose we have wish to simulate a Lévy process with increment distribution $F(x;\boldsymbol{\theta})$ over the time period $[0, T]$ and the process is observed every Δt time units.

Algorithm 2 Simulating a Lévy Jump-Diffusion (Via Increment Distribution)

Generate $T/\Delta t$ random variables $L_i \sim F(x;\boldsymbol{\theta})$
return The cumulative sum of (0, $\boldsymbol{L}$)

In both cases we specify and simulate the driving process X_t which can be converted to a price series using the fact that:

$$S_t = S_0 e^{X_t}$$

2.3 Fitting Lévy Models to Share Price Data

For most exponential Lévy models, we do not have an expression for the transitional density of the driving process making parameter estimation by direct maximum likelihood estimation (MLE) infeasible. However, due to the Lévy-Khintchine Formula 2.2, we can obtain a characteristic function for any given Lévy process. We thus use the characteristic function as a basis for any estimation approach. Where our analysis pertains to equity shares we use Tesla and Goldman Sachs for illustrative examples and comparisons of fit, the daily log returns for which can be seen in Figure 2.1. We note that where Tesla displays a return series which is more volatile - indicated by many extreme deviations relative to Goldman Sachs - we expect the jump-diffusion model to outperform Black-Scholes.

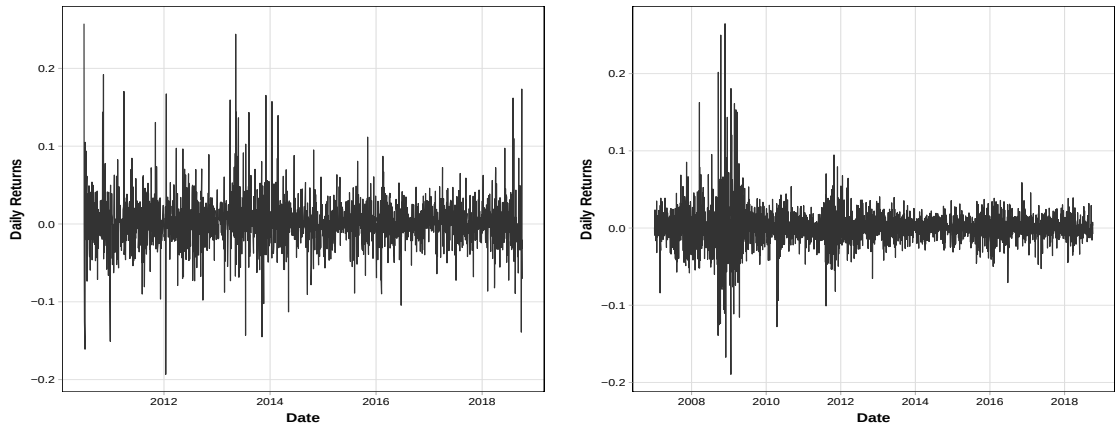

(a) Tesla (b) Goldman Sachs

FIGURE 2.1: Return series for Tesla and Goldman Sachs

2.3.1 Empirical Characteristic Function Estimation

This estimation procedure, presented by Jun Yu in [16], is based on the idea of selecting the parameter set which minimizes the distance between the empirical characteristic function of the data and the characteristic function of the desired model.

Justification for such a method stems from the fact that the Fourier transform of the probability density function generates the characteristic function providing a clear one-one correspondence between the CF and the distribution of interest [16].

Suppose the cumulative density function (CDF) of X is $F(x;\boldsymbol{\theta})$ which depends on a K-dimensional vector of parameters $\boldsymbol{\theta}$. The characteristic function can be defined by Equation 2.7

$$c(r;\boldsymbol{\theta}) = \mathbb{E}[\exp(irX)] = \int \exp(irx)dF(x;\boldsymbol{\theta}) \tag{2.7}$$

We can therefore define the empirical characteristic function (ECF) as

$$c_n(r) = \frac{1}{n}\sum_{j=1}^{n}\exp(irX_j), \tag{2.8}$$

where $i^2 = -1$, $\{X_j\}_{j=1}^n$ is an iid. sequence, r is the transform variable.

Yu goes on to point out that the ECF estimator can be treated as a generalised method of moments (GMM) estimator where GMM is sub-optimal to maximum likelihood estimation (MLE).

In our implementation of ECF estimation we compute the ECF estimator, which we denote by $\hat{\boldsymbol{\theta}}_{ECF}$, as:

$$\hat{\boldsymbol{\theta}}_{ECF} = \arg\inf_{\hat{\boldsymbol{\theta}}} \int_{\mathbb{R}} |c_n(r) - c(r;\boldsymbol{\theta})|^2 w(r)dr \tag{2.9}$$

Where $w(r)$ is a continuous waiting function. We pick $w(r) = e^{-r^2}$ to ensure the integrand is integrable and the objective function is well behaved for purposes of numerical optimization. We motivate our use of this weighting function using the fact that most

of the information regarding the parameter vector is contained around the centre of the characteristic function. It is worth noting that, as discussed in [16], the ECF estimator is in general less efficient than the MLE. The ECF estimator can achieve MLE efficiency with appropriately chosen $w(r)$, however, selecting the appropriate $w(r)$ requires the distribution function of the data which is generally not known in our application.

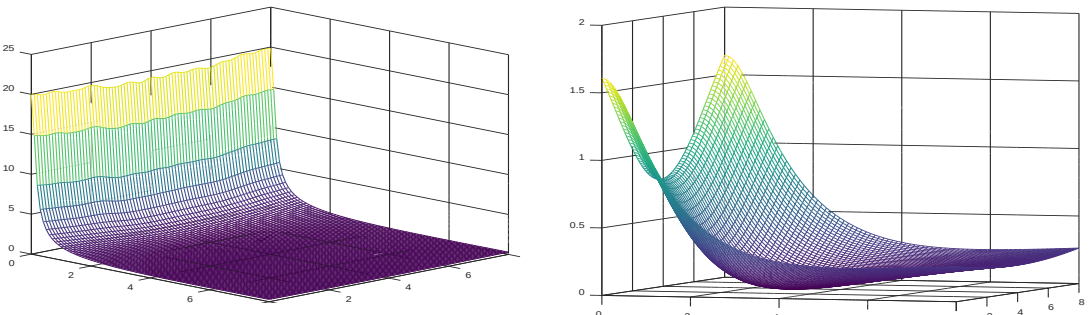

(a) Unweighted Objective (b) Weighted Objective

FIGURE 2.2: ECF objective surfaces for approximation of normal distribution parameters $\mu = 4, \sigma = 3$

2.3.2 Maximum Likelihood Estimation via Fourier-Cosine Series Expansions

In their paper [4], Fang and Oosterlee present a method for pricing European options based on computing the cosine expansion of the inverse Fourier integral. They name this pricing methodology the COS method. The paper goes on to describe methodology for approximating an unknown density function $f_X(x)$ using its Fourier cosine expansion and characteristic function $\phi_X(u)$.

The characteristic function of some random variable X with density function $f_X(x)$ is defined as:

$$\phi_X(u) = \mathbb{E}[e^{iux}] = \int_{-\infty}^{\infty} e^{iux} f_X(x) dx. \tag{2.10}$$

A random variable X is absolutely continuous if and only if the characteristic function of that random variable $\phi_X(u)$ is integrable. If this is the case the probability distribution function of X, $f_X(x)$ exists and can be easily recovered via the inverse Fourier transform

$$f_X(x) = \frac{1}{2\pi} \int_{-\infty}^{\infty} e^{-iux} \phi_X(x) dx. \tag{2.11}$$

Where the Fourier cosine expansion of a function $f(x)$ with domain $[a, b] \in \mathbb{R}$ is given by;

$$f(x) = \frac{1}{2} A_0 + \sum_{k=1}^{\infty} A_k \cos\left(k\pi \frac{x-a}{b-a}\right), \tag{2.12}$$
$$\text{with } A_k = \frac{2}{b-a} \int_a^b f(x) \cos\left(k\pi \frac{x-a}{b-a}\right).$$

This expansion exists for any real function within a bounded domain. Although our density functions are defined over all real numbers, the fact that they are non-negative and must have a finite integral implies that they tend to zero in the limits. Thus we can pick

a suitable interval $[a,b] \in \mathbb{R}$ to restrict our function without a loss in accuracy. We also cannot compute the sum in 2.12 to infinity, so we further approximate $f(x)$ by taking the sum of the first $N-1$ terms for some suitable chosen N.

Taking the Fourier cosine expansion of 2.11 with these approximations leads us to the following formula:

$$f_X(x) \approx \frac{1}{2}A_0 + \sum_{k=1}^{N-1} A_k \cos\left(k\pi\frac{x-a}{b-a}\right), \tag{2.13}$$
$$\text{where } A_k = \frac{2}{b-a}\Re\left\{\phi_X\left(\frac{k\pi}{b-a}\right)e^{-i\frac{ka\pi}{b-a}}\right\}.$$

Formula 2.13 gives us a way of recovering the density of the log returns of a given share whose price process we modelled with an exponential Lévy process. In order to obtain maximum likelihood estimates for the parameters in the driving process, we use Formula 2.13 to construct a log-likelihood function.

For the purposes of density recovery and likelihood estimation we have found that the truncation range $[a,b]$ should be chosen such that as much of $f(x)$'s total area is contained on $[a,b]$. A larger range does however require greater values of N to produce an accurate approximation so computational feasibility should be considered when selecting $[a,b]$. For this reason we recommend selecting the smallest interval $[a,b]$ such that $\int_a^b f_X(x) \geq 1-|\epsilon|$ where ϵ is some acceptable error threshold.

Density Recovery - Normal Distribution
We test the approximation given in 2.13 by applying it to the standard normal density. Table 2.1 shows the values of the normal density evaluated at the given x values against the COS approximation for various values of N, the number of terms in the sum.

	x				
Function	-1	-0.5	0	0.5	1
True Density	0.2419707	0.3520653	0.3989423	0.3520653	0.2419707
Approximation $N=5$	0.2608806	0.3296038	0.3549819	0.3296038	0.2608806
Approximation $N=10$	0.2435455	0.3521240	0.3973266	0.3521240	0.2435455
Approximation $N=20$	0.2419707	0.3520653	0.3989423	0.3520653	0.2419707

TABLE 2.1: Recovery of Standard Normal Density

As can be seen from the table, the COS approximation converges fairly quickly, having near 0 error at just 20 terms. See Figure 2.3 for a plot of the approximate density against the exact density for various values of N.

Density Recovery - Brownian Motion with Normal Jumps
We now test the COS approximation for the density of the increments of the Lévy jump-diffusion $X_t = \mu t + \sigma B_t + \sum_{i=1}^{N_t} Y_i$ where $Y_i \overset{iid.}{\sim} N(m,\delta)$. The density of X_1 is not known in closed form so we can not compare the COS approximation to the true density, however a quickly converging series approximation based on the law of total probability[15] is given

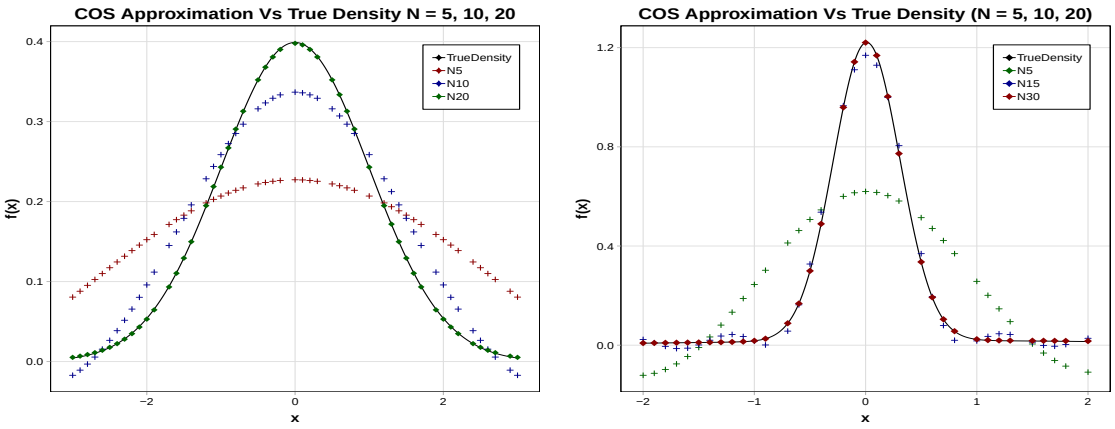

(a) Standard Normal

(b) Brownian Motion with Normal Jumps

FIGURE 2.3: COS Approximation of Standard Normal and Brownian Motion with Normal Jumps For Various N

by:

$$f(x) = e^{-\lambda} \sum_{k=0}^{\infty} \frac{\lambda^k \exp\left[-\frac{(x-\mu-km)^2}{2(\sigma^2+k\delta^2)}\right]}{k!\sqrt{2\pi(\sigma^2+k\delta^2)}}. \tag{2.14}$$

We compare the COS approximation for the density of X_1 with 2.14 where we take the first one hundred terms of the sum. Figure 2.3 illustrates the COS approximation against 2.14. From this figure we note that the COS approximation converges near $N = 30$ terms.

Maximum Likelihood Estimation

To find MLE estimates for our parameters we make use of Equation 2.13 to generate an approximate density $\hat{f}_X(x)$ for $f_X(x)$. We then use this density to construct an approximate likelihood function for our data.

$$L(\boldsymbol{x};\boldsymbol{\theta}) = \prod_{i=1}^{n} \left[\frac{1}{2}A_0 + \sum_{k=1}^{N-1} A_k \cos\left(k\pi\frac{x_i - a}{b-a}\right)\right], \tag{2.15}$$

$$\ln(L(\boldsymbol{x};\boldsymbol{\theta})) = \sum_{i=1}^{n} \ln\left[(b-a) + \sum_{k=1}^{N-1} A_k \cos\left(k\pi\frac{x_i - a}{b-a}\right)\right]. \tag{2.16}$$

The numerical derivative of 2.16 was seldom well behaved so we decided to use gradient free optimization algorithms in order to maximise the log-likelihood, namely Nelder and Meads downhill simplex method. This resulted in a computationally expensive optimisation procedure, we saw up to twelve hour runtimes when estimating our parameters. To improve the efficiency of our estimation procedure we made the following changes: Let $\boldsymbol{A_\theta} = \begin{bmatrix}(b-a) & A_1 & A_2 & \cdots & A_{N-1}\end{bmatrix}^T$,

$$\text{Let } \boldsymbol{C_x} = \begin{bmatrix} 1 & 1 & \cdots & 1 \\ cos\left(1\pi\frac{x_1-a}{b-a}\right) & cos\left(1\pi\frac{x_2-a}{b-a}\right) & \cdots & cos\left(1\pi\frac{x_n-a}{b-a}\right) \\ cos\left(2\pi\frac{x_1-a}{b-a}\right) & cos\left(2\pi\frac{x_2-a}{b-a}\right) & \cdots & cos\left(2\pi\frac{x_n-a}{b-a}\right) \\ \vdots & \vdots & \vdots & \vdots \\ cos\left((N-1)\pi\frac{x_1-a}{b-a}\right) & cos\left((N-1)\pi\frac{x_2-a}{b-a}\right) & \cdots & cos\left((N-1)\pi\frac{x_n-a}{b-a}\right) \end{bmatrix}.$$

We use the subscripts on $\boldsymbol{\theta}$ and $\boldsymbol{x}$ to make explicit that the matrix $\boldsymbol{A_\theta}$ depends on the parameter vector but not the observations and $\boldsymbol{C_x}$ depends on the observations but not the parameter vector. Using these matrices 2.16 becomes

$$\ln(L(\boldsymbol{x};\boldsymbol{\theta})) = \mathbf{1}^T \ln\left(\boldsymbol{C_x^T} \times \boldsymbol{A_\theta}\right), \tag{2.17}$$

where $\ln(\boldsymbol{v}) = \{\ln v_i\}$ for a vector $\boldsymbol{v} = \{v_i\}$. Apart from the performance improvements due to vectorisation, 2.17 also has the added benefit that, when using a numerical maximiser $\boldsymbol{C_x}$ only has to be evaluated once since it does not depend on the parameter vector and our maximiser would only need to re-evaluate $\boldsymbol{A_\theta}$. These changes resulted in our estimation procedure producing estimates in five minutes in the most extreme cases we attempted.

2.3.3 Comparison of Estimation Procedures

To evaluate the performance of the estimation approaches above we simulate various Lévy jump-diffusions with fixed true parameter vector $\boldsymbol{\theta}_0$. We simulate each process N times and for each simulation we numerically compute the MLE-COS estimate $\hat{\boldsymbol{\theta}}_{COS}$ and the ECF estimate $\hat{\boldsymbol{\theta}}_{ECF}$. This allows us to obtain empirical sampling distributions for the two estimators as well as construct confidence intervals for the parameters. We use the results to examine the biases and variances of $\hat{\boldsymbol{\theta}}_{COS}$ and $\hat{\boldsymbol{\theta}}_{ECF}$.

Experiment 1: Brownian Motion with Drift

In the first experiment we use the following Lévy process,

$$X_t = \mu t + \sigma B_t.$$

The corresponding exponential Lévy for this driving process is geometric Brownian motion. We fix a single day as one time unit and thus under this process the daily log returns have the distribution $X_1 \sim N(\mu, \sigma^2)$. We simulate $n = 3000$ days/observations of this process with; $\mu = 0.04$, $\sigma = 0.2$ and $N = 1000$ sample paths for this process.

	Statistic				
Parameter	$\boldsymbol{\theta}_0$	$\hat{\boldsymbol{\theta}}_{COS}$	$\hat{\boldsymbol{\theta}}_{ECF}$	$Conf_{0.95}(\hat{\boldsymbol{\theta}}_{COS})$	$Conf_{0.95}(\hat{\boldsymbol{\theta}}_{ECF})$
μ	0.04	0.0399	0.0403	[0.0329, 0.0473]	[0.0331, 0.0475]
σ	0.20	0.1999	0.1999	[0.1949, 0.2047]	[0.1950, 0.2050]

TABLE 2.2: Experiment 1 Results

Table 2.2 illustrates the results of Experiment 1. Both ECF and MLE-COS estimation produced point estimates that are within 1% of the true parameter values. Between the two approaches we observe 95% confidence intervals of equivalent width for the μ parameter,

however, the COS estimate interval is slightly narrower than that of the ECF estimate for σ.

Experiment 2: Brownian Motion with Normal Jumps

We use the following Lévy process

$$X_t = \mu t + \sigma B_t + \sum_{i=1}^{N_t} Y_i,$$

where $Y_i \overset{iid.}{\sim} N(m, \delta)$. The corresponding exponential Lévy model is the asset price model presented by Merton in his option pricing framework [9]. Under this model the distribution of daily log returns is not known in closed form.

We simulate $n = 3000$ observations of this process with $\mu = 0.05$, $\sigma = 0.25$, $\lambda = 0.4$, $m = 0.5, \delta = 1.4$ for $N = 1000$ sample paths.

		Statistic			
Parameter	$\boldsymbol{\theta}_0$	$\hat{\boldsymbol{\theta}}_{COS}$	$\hat{\boldsymbol{\theta}}_{ECF}$	$Conf_{0.95}(\hat{\boldsymbol{\theta}}_{COS})$	$Conf_{0.95}(\hat{\boldsymbol{\theta}}_{ECF})$
μ	0.05	0.0496	0.0502	$[0.0343, 0.0643]$	$[0.0297, 0.0731]$
σ	0.25	0.2499	0.2552	$[0.2359, 0.2654]$	$[0.1675, 0.3209]$
λ	0.40	0.4011	0.4084	$[0.3549, 0.4507]$	$[0.3247, 0.4926]$
m	0.50	0.5172	0.5009	$[0.3749, 0.7528]$	$[0.3722, 0.6159]$
δ	1.40	1.4122	1.3699	$[1.2744, 1.5799]$	$[1.2437, 1.5283]$

TABLE 2.3: Experiment 2 Results

Table 2.3 shows the numerical results for Experiment 2. We note that both estimation procedures produce point estimates all within 5% of the true parameter value. The MLE-COS procedure produces more accurate point estimates and displays narrower confidence intervals for the parameters (μ, σ, λ). Whereas the ECF estimate produces a more accurate point estimate and narrower confidence intervals for the jump distributions' parameters (m, δ).

Experiment 3: Brownian Motion with Lévy alpha-stable Jumps

Here we simulate the Lévy process

$$X_t = \mu t + \sigma B_t + \sum_{i=1}^{N_t} L_i,$$

where L_i are iid. random variables from the Lévy alpha-stable distribution with parameters $\alpha, \beta, \gamma, \delta$. We pick this jump distribution in order to explore how the estimation procedures fare under a larger parameter vector and when the process has a jump component with infinite variance. We use the stable distribution parametrisation where the characteristic function of the L_i is given by;

$$\phi_L(u;\alpha,\beta,\gamma,\delta) = \begin{cases} \exp\left\{ iu\delta - |\gamma u|^\alpha \left[1 - i\beta sign(u)(|\gamma u|^{1-\alpha} - 1)\tan\left(\frac{\pi\alpha}{2}\right)\right]\right\} & \alpha \neq 1 \\ \exp\left\{ iu\delta - |\gamma u|^\alpha \left[1 + i\beta sign(u)\frac{2}{\pi}\log|\gamma u|\right]\right\} & \alpha = 1 \end{cases} \tag{2.18}$$

Where $\alpha \in [0,2], \beta \in [-1,1], \gamma \in [0,\infty), \delta \in \mathbb{R}$. Plugging this into 2.3 yields the characteristic function of X_t, which we then use to perform the parameter estimation procedure.

We simulate this process for n = 3000 observations with $\mu = 0.06$, $\sigma = 0.4$, $\lambda = 0.2$, $\alpha = 1.4$, $\beta = 0.2$, $\gamma = 0.1$, $\delta = 0.3$. For $N = 1000$ sample paths.

For this process the ECF objective is divergent and we are unable to obtain ECF parameter estimates. COS-MLE estimates can still be obtained, however, as can be seen from Table 2.4, these estimates are unreliable. Confidence intervals for each parameter are very wide and for the α parameter, despite taking up half of the feasible range of α the confidence interval does not even contain the true value.

	Statistic		
Parameter	$\boldsymbol{\theta}_0$	$\hat{\boldsymbol{\theta}}_{COS}$	$Conf_{0.95}(\hat{\boldsymbol{\theta}}_{COS})$
μ	0.06	0.1118	[0.0104, 0.1447]
σ	0.40	0.4258	[0.3941, 0.7755]
λ	0.20	0.0243	[0.0000, 0.2409]
α	1.40	0.5085	[0.0000, 0.9988]
β	0.20	0.0204	[−0.8233, 1.0000]
γ	0.10	0.0407	[0.0000, 1.0331]
δ	0.30	0.0162	[−1.1171, 1.7851]

TABLE 2.4: Experiment 3 Results

Concluding Remarks In the process of implementing our experiments we observed the following:

- Estimation of Lévy jump-diffusions are unreliable when λ, the jump rate is small (<0.05). The effect of this can be mitigated by using a year as a single time unit, this effectively rescales lambda to a per-annum jump rate which ensures a $\lambda > 0.05$ for all shares we fit.
- Estimation of the parameters is unreliable when the drift component of the diffusion is close to the mean of the jump distribution. Again we have found that this can be mitigated by setting a year as the time unit, thus rescaling the drift without effecting the jump distributions parameters.
- If the characteristic function of the Lévy jump-diffusions is not integrable (an example of such a case is when the jump sizes are constant), then it's density does not exist and COS estimation will produce erroneous estimates, for this case we would recommend the use of ECF estimation.

Because of these results we would recommend that for practical application of Lévy jump-diffusions, a time unit of at least 1 month is selected.

Figure 2.4 shows the daily log returns of Tesla shares against the density implied by the Merton model, Kou model and the density implied by the Black-Scholes model. All parameters were estimated using MLE-COS. Lévy jump-diffusions produce a significantly better fit on the daily log returns than the normal distribution implied by the Black-Scholes model. We see the biggest improvement in fit when including jumps, however, selecting the jump-distribution as a distribution which is more leptokurtic appears to have a marginal improvement. We also note that where the underlying asset displays few jumps the models do not necessarily fit much better.

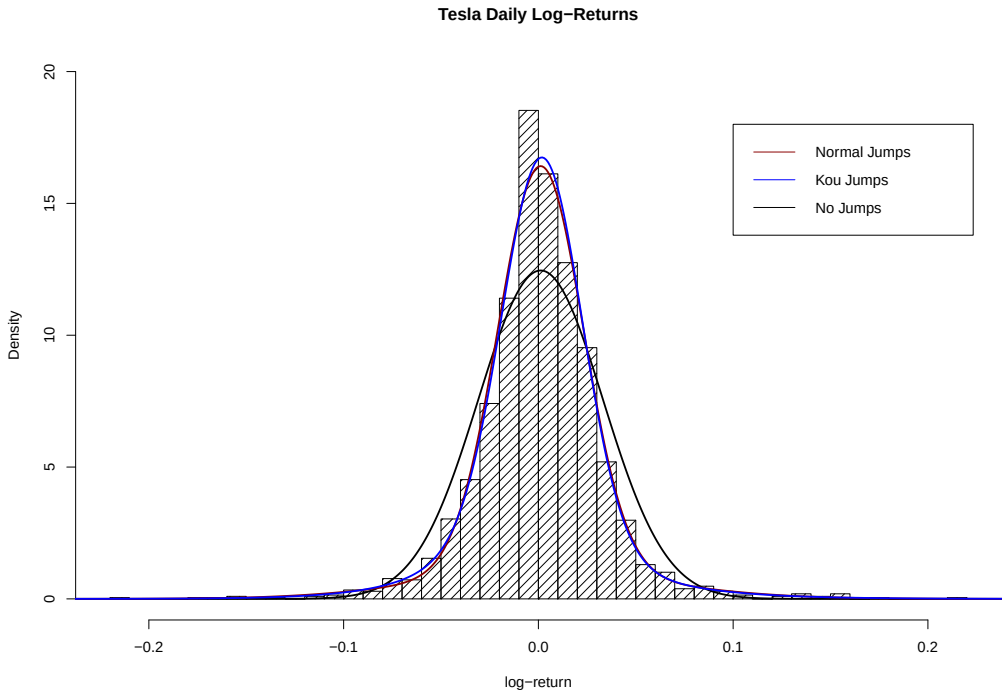

FIGURE 2.4: Daily Log Return Densities of Various Lévy Jump-Diffusions fit to Tesla shares.

Chapter 3

Option Pricing under Lévy Jump-Diffusion Processes

One of the main criticisms against Black-Scholes option pricing is that the volatility implied by the Black-Scholes model is constant with respect to the strike price and time till maturity of an option and is equal to the standard deviation of the returns of the underlying asset. However, this has been shown to be empirically false. A key advantage of Lévy jump-diffusions over Black-Scholes for option pricing is that the volatility implied by Lévy jump-diffusion models is dependent on both the strike and time till maturity of the option and is not equal to the historical volatility of the underlying [15].

3.1 Modelling Asset Prices Under the Risk Neutral Measure

Previously we modelled the asset price process S_t under the real world measure $\mathbb{P}$ using the exponential Lévy model

$$S_t = S_0 e^{L_t}.$$

Where L_t is a Lévy jump-diffusion with Lévy triplet $(\mu, \sigma, \lambda F(x))$. For the purposes of option pricing we must model the asset price process under the risk-neutral measure $\mathbb{P}^*$. We apply the exponential Lévy model in this case as well but with Lévy triplet $(\mu^*, \sigma^*, \lambda^* F(x))$. Where $\mathbb{P}^*$ and $\mathbb{P}$ are equivalent measures and L_t's first moment and first exponential moment are finite.

Since $\mathbb{P}^*$ is the risk-neutral measure the process $\{e^{(\delta-d)t} S_t\}_{t\geq 0}^T$ must be a $\mathbb{P}^*$-martingale [10]. Where $\delta \geq 0$ is the risk-free force of interest and $d \geq 0$ is the continuous dividend yield of the asset. In order for $\{e^{(\delta-d)t} S_t\}_{t\geq 0}^T$ to be a martingale the drift term must satisfy;

$$\mu^* = \delta - d - \frac{1}{2}\sigma^{*2} - \lambda^* \big(\mathbb{E}[e^x - 1] - \mathbb{E}[x]\big) \tag{3.1}$$

In theory one can apply Girsanov's theorem to transform the discounted price process under the real world measure to a process under the risk-neutral measure. Exploiting a special case of the theorem ensures that the new process is also a Lévy process, where the two Lévy triplets exhibit the following relationship;

1. $(\sigma^*)^2 = \sigma^2$,
2. $\lambda^* = Y\lambda$,
3. $\mu^* = \mu + \sigma^2\beta + \lambda(Y-1)\mathbb{E}[x]$,

where (β, Y) is deterministic and independent of time.

The implication of this result, by the fundamental theorem of asset pricing, is that the market is not complete under Lévy jump-diffusions [15].

3.2 The Black-Scholes Option Pricing Formula

Solving Equation 1.2 from Chapter 1 would yield the option pricing formula under Black-Scholes Merton given by Equation 3.2 below. It is easy to see why the Black-Scholes model is so popular, the formula is tractable and as such lends itself to "plug-and-play" results without any prior knowledge of the statistical assumptions made.

$$C(S,t) = SN(d_1) - Ke^{-r(T-t)}N(d_2) \tag{3.2}$$

$N(.)$ is CDF of the normal distribution

$$d_1 = \frac{\ln\left(\frac{S}{K}\right) + \left(r^2 + \frac{\sigma^2}{2}\right)(T-t)}{\sigma\sqrt{T-t}}$$

$$d_2 = d_1 - \sigma\sqrt{T-t}$$

3.3 Option Pricing via Fourier Transform

Suppose we are not able to solve the stochastic differential equation describing the return distribution. We note that for the class of Lévy jump-diffusions we can always find the characteristic function, as such we are interested in option valuation that relies on the availability of a characteristic function describing the logarithm of the stock price. In this case, where closed formulas are no longer available, a fast deterministic algorithmic technique for option pricing based on Fourier inversion [3] is used. Carr-Madan inversion gives the call price $C_T(k)$ of a vanilla option to be the inverse Fourier transform of $\psi_T(v)$ to be,

$$C_T(k) = \frac{e^{-\alpha k}}{\pi}\int_0^\infty \Re\left[e^{-ivk}\psi_T(v)\right]dv, \tag{3.3}$$

$$\psi_T(v) = \frac{e^{-rT}\phi_T[v-(\alpha+1)i]}{\alpha^2+\alpha-v^2+i(2\alpha+1)v}. \tag{3.4}$$

Where; $i^2 = -1$, $\phi_T(.)$ is a charactersitic function of the log-asset price ,
r is the force of interest rate, T is the time to maturity (annualised),
k is the logarithm of the strike $\log(K)$, α is an arbitrarily robust constant.

As this method relies on the characteristic function of the natural logarithm of the spot price $\psi_{log(S_t)}(v)$ we must first derive this function. Suppose X_t is a Lévy process and we model the asset price using an exponential Lévy model $S_t = S_0\exp\{X_t\}$. From the Lévy-Khintchine 2.2 we have $\psi_{X_t}(v)$ the characteristic function of the driving process.

Taking the logarithm of both sides of the exponential Lévy model we obtain

$$\log(S_t) = \log(S_0) + X_t.$$

Then by computing the expectation $\mathbb{E}[\exp\{iv\log(S_t)\}]$ we get

$$\begin{aligned}\psi_{log(S_t)}(v) &= \mathbb{E}[\exp\{iv\log(S_t)\}] \\ &= \mathbb{E}[\exp\{iv\log(S_0) + ivX_t\}] \\ &= \exp\{iv\log(S_0)\}\mathbb{E}[\exp\{ivX_t\}] \\ &= \exp\{iv\log(S_0)\}\psi_{X_t}(v)\end{aligned}$$

Thus we have a general expression for $\psi_{log(S_t)}(v)$ whenever X_t is a Lévy jump-diffusion, given by:

$$\psi_{log(S_t)}(v) = \exp\left\{iv\log(S_0) + t\big(i\gamma u - \frac{\sigma^2u^2}{2} + \lambda\int_{\mathbb{R}}(e^{iux}-1)f(dx)\big)\right\}. \tag{3.5}$$

Here the characteristic function is evaluated for a risk neutral price process and the formula is valid for pricing at-the-money and in-the-money options [3]. To use Carr-Madan to price put options we obtain call option prices at specified maturities and strikes and apply put-call-parity[1] to convert these to put option prices.

3.4 Option Pricing via The COS Method

Here we present the COS method for option pricing as detailed by Fang and Oosterlee in [4]. Let $V(S_t,t)$ be the price at time t of a European option on an asset S with payoff function h and maturity time T. Therefore

$$V(S_t,t) = e^{-r(T-t)}\mathbb{E}^*[h(S_T)],$$

suppose now that we are pricing a European call with strike price K and maturity time T. This option will have payoff function $h(S_T) = \max(S_T - K, 0)$. We wish to compute $\mathbb{E}^*[h(S_T)]$ the expected pay off of the option under the risk neutral measure. S_T is a function of the driving process L_T whose density function is usually unknown. However, this process is a Lévy process and, as per Lévy-Khintchine 2.2, we have the characteristic function for any Lévy process. This makes the COS method an attractive procedure because it allows us to compute the expectation of the pay-off function provided that we have the characteristic function of the log returns.

The COS option pricing formula is based on approximation the value function $V(S_t,t)$, with its fourier-cosine expansion as explained in 2.3.2. The formula is given by

$$V(S_t,t) \approx e^{-r(T-t)}\Big(\frac{1}{2}\mathcal{V}_0\phi_{X_{T-t}}(0) + \sum_{k=1}^{N-1}\Re\left\{\phi_{X_{T-t}}\Big(\frac{k\pi}{b-a}\Big)e^{-i\frac{ka\pi}{b-a}}\right\}\mathcal{V}_k\Big), \tag{3.6}$$

where X_{T-t} is the driving process of the exponential Lévy model under the risk neutral measure at time $T-t$ and $\phi_{X_{T-t}}$ is its characteristic function. The sequence $\{\mathcal{V}_k\}$ depends on the pay-off function h but can be computed analytically for plain vanilla and digital options [4]. For European call and put options Fang and Oosterlee present the following

[1] A formula that relates call prices to put prices for options with the same strike, maturity and underlying.

analytical expressions for $\{\mathcal{V}_k\}$;

$$\mathcal{V}_k^{\text{call}} = \frac{2}{b-a} K(\chi_k(0,b) - \varphi_k(0,b)), \tag{3.7}$$

$$\mathcal{V}_k^{\text{put}} = \frac{2}{b-a} K(-\chi_k(a,0) + \varphi_k(a,0)), \tag{3.8}$$

$$\text{where } \chi_k(c,d) = \frac{1}{1+\left(\frac{k\pi}{b-a}\right)^2}\left[\cos\left(k\pi\frac{d-a}{b-a}\right)e^d - \cos\left(k\pi\frac{c-a}{b-a}\right)e^c + \right.$$
$$\left. \frac{k\pi}{b-a}\sin\left(k\pi\frac{d-a}{b-a}\right)e^d - \frac{k\pi}{b-a}\sin\left(k\pi\frac{c-a}{b-a}\right)e^c\right],$$

$$\varphi_k(a,b) = \begin{cases} \left[\sin\left(k\pi\frac{d-a}{b-a}\right) - \sin\left(k\pi\frac{c-a}{b-a}\right)\right]\frac{b-a}{k\pi} & k \neq 0 \\ (d-c) & k = 0 \end{cases}$$

For a detailed derivation of the above see [4]. It should be noted that the COS method produces severe errors when used to price out of the money calls, for this reason Fang and Oosterlee advise pricing the puts and obtaining the call prices using put-call-parity.

3.5 Model Calibration for Lévy Jump-Diffusions

Both option pricing methodologies we have presented are dependent on the parameters of the asset price model which we will denote by $\boldsymbol{\theta}$. We will calibrate our Lévy jump-diffusion models by minimizing the distance between our pricing function and market vanilla option prices as described in [15]. This objective is defined as

$$\hat{\boldsymbol{\theta}} = \arg\inf_{\boldsymbol{\theta}} \sum_{i=1}^{N} w_i (P_i^{obs} - P^{\boldsymbol{\theta}}(T_i, K_i))^2. \tag{3.9}$$

Where P^{obs} are the observed market prices and $P^{\boldsymbol{\theta}}(T_i, K_i)$ is the price returned by our pricing function. We use weights $w_i = (P_i^{obs})^{-2}$ to scale all terms in the objective to the same magnitude. We choose to calibrate on two shares, Tesla and Goldman Sachs as these stocks are in different sectors and presently have option data available. We also choose to calibrate on time to maturities of 5, 30 and 55 days which are annualised.

3.5.1 Parameters for Option Pricing

By optimising the objective given by Equation 3.9 we obtain parameter estimates under each of the two option pricing methods. First we specify a σ parameter under each objective, where σ represents the estimated diffusion parameter under the real world measure, we use $\hat{\sigma}$ estimated from 2.17 as an estimator for σ. This σ is uniquely optimised for each asset we wish to model and is obtained in this way because, by Girsanov's theorem, the diffusion component is the same under both the real world and the risk neutral measure. We compare the price estimates from Carr-Madan and the COS method when utilising the characteristic function under the risk neutral measure (an equivalent martingale measure $\mathbb{P}^*$ such that the discounted price $\hat{S}_t$ is a martingale) for the Merton jump-diffusion model given by;

$$
\begin{aligned}
\mathbb{P}^* : S_t &= S_0 \exp\left[\mu^M t + \sigma W_t^M + \sum_{i=1}^{N_t} Y_i\right], \\
\mathbb{P}^* : \mu^M &= r - \frac{\sigma^2}{2} - \lambda \mathbb{E}\left[e^{Y_i} - 1\right] \\
&= r - \frac{\sigma^2}{2} - \lambda \mathbb{E}\left[\exp\left(m + \frac{\delta^2}{2}\right) - 1\right], \\
\mathbb{P}^* : \psi_t^M(u) &= \exp\left\{iut\mu^M - \frac{t(\sigma u)^2}{2} + t\lambda\left(e^{\left(miu - \frac{(\delta u)^2}{2}\right)} - 1\right)\right\},
\end{aligned} \tag{3.10}
$$

to the prices obtained under Black-Scholes formula 3.2 with σ equal to the historical volatility (annualised standard deviation of the asset return series). Table 3.1 shows the parameter estimates for 3.10 acquired from calibration on the Goldman Sachs underlying share price and market data, we obtain the same estimates for the calibration under both Carr-Madan and the COS pricing methods. The optimisation technique used is the Nelder-Mead downhill simplex, as it is more computationally stable than the LBFGS-B. We also observe that the COS estimation procedure is more computationally efficient than the Carr-Madan formulation which evaluates the integral proposed by 3.3 as opposed to using the FFT algorithm in [3]. We choose to sacrifice the efficiency of FFT for accuracy in the Carr-Madan formula as the FFT relies on two constraints; firstly, the strikes must be placed at an equal distance in the log space and secondly, the Nyquist relation $\Delta k \Delta w = 2\pi/N$ must also be obeyed. As the FFT requires equidistant integration it is restricted to utilising simple quadrature rules in order to recover option prices offering justification for the use of 3.3 to recover original call price without cleaning the data used to calibrate our models.

	Parameter Value		
Time	λ	μ	δ
$t = 5/250$	0.00516	0.18940	0.56378
$t = 30/250$	0.70747	0.00063	0.00016
$t = 55/250$	0.79237	0.00062	0.00034

TABLE 3.1: Parameter Estimates for Merton Characteristic Function obtained from Model Calibration with $(\sigma = 0.28505)$.

3.5.2 Pricing in a Black-Scholes Market and with Jumps (Merton Model)

By setting the parameter values of the characteristic equal to those obtained from the calibration we can plot the model fits against the data, this is illustrated in Figure 3.1.

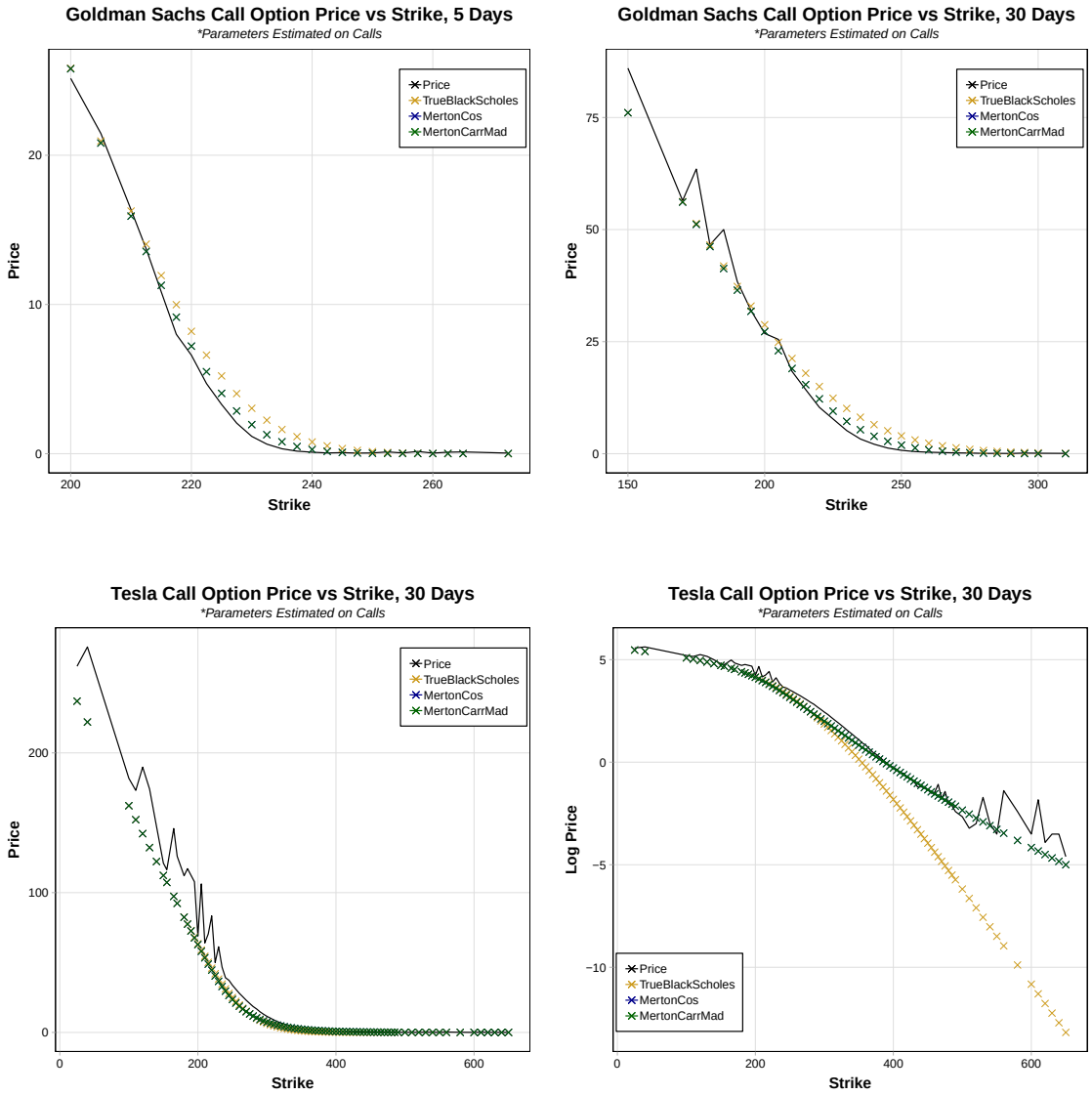

FIGURE 3.1: Post Calibration Call Prices at Various Times to Maturity

We see that for all the fits both Carr-Madan and COS methods produce superimposed fit of the Merton jump model which incidentally also appears to be better fit to the data. Where the TSLA 30 days until maturity call prices seem to be overlaid between Black-Scholes and the Merton jump model we can display the price series on the log-scale. This yields the curve on the bottom right, where we can clearly see the Black-Scholes prices diverge from the Merton jump model prices which are evidently a better fit to the market data. This example is in-line with our initial hypothesis - that the jump-diffusion pricing model should better fit the "jumpier" shares - as the Lévy jump-diffusion process applies the characteristics of the jump distribution to the base model of geometric Brownian motion to better capture the extreme events observed in financial data.

We can examine the behaviour of our estimation and pricing methods for longer maturities, in this case 173 days until maturity for Tesla shows that, unlike before, the COS and Carr-Madan techniques give different parameter estimates for $\hat{\theta}$. These estimates are given in Table 3.2 below, we see that for longer maturities the mean jump size tends to increase while the jump intensity decreases with the length of the holding period. This behaviour

is similar to that observed by [15].

	Parameter Value		
Method	λ	μ	δ
$\boldsymbol{\theta}_{COS}$	51.04612	0.05537	0.00895
$\boldsymbol{\theta}_{Carr}$	94.67224	0.04165	0.00316

TABLE 3.2: Parameter Estimates for Merton Characteristic Function obtained from Model Calibration with $(\sigma = 0.3482813)$ for 173 days until maturity.

Figure 3.2 displays the longer time to maturity call option on the more volatile asset (Tesla). On the left the prices are difficult to distinguish, as such we plot the prices on the log-scale (right). What is clear is that the Merton jump model again outperforms plain Black-Scholes, however, where the COS and Carr-Madan now produce differing parameter estimates it is unclear as to which method is more accurate as Carr-Madan appears to best fit up until a strike $(K = 460)$ after which the COS method appears to lay closer to the market data line. Further analysis would need to be done on longer term options to explore the key differences in the two methods. Although both Carr-Madan and COS produce the same prices when given the same parameter values, we found that there were cases where the objective calibrated to a more optimal solution when using Carr-Madan.

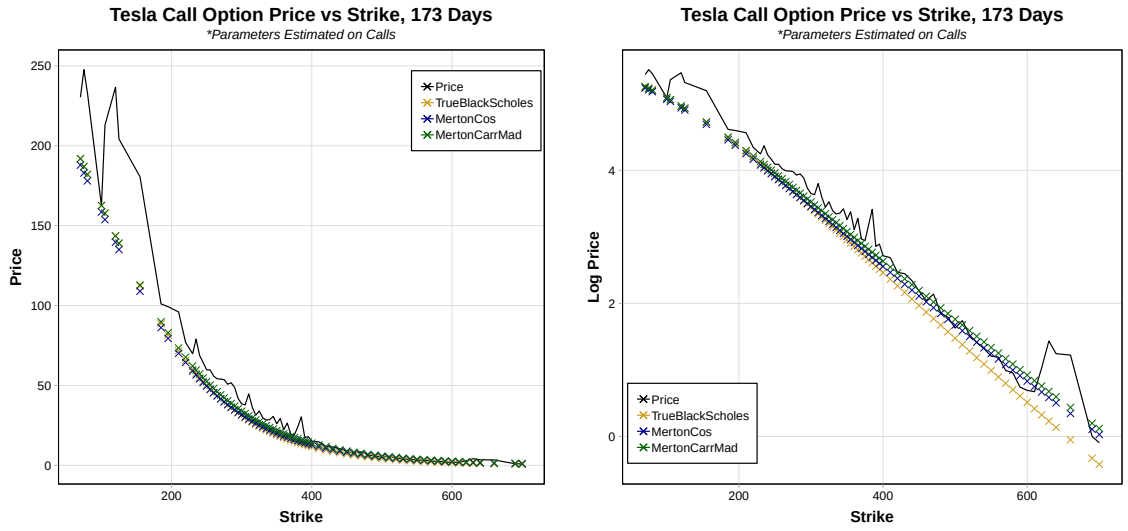

FIGURE 3.2: Market Prices vs Estimated Prices and Vanilla Black-Scholes Formula for Longer Term Tesla

3.5.3 Pricing Put Options

Consider the construction of another option comprised of a strike, time to maturity and underlying asset price. Data for such options (barrier, digital, lookback etc.) is not readily available to test the accuracy of pricing "out-of-sample" options using the procedures developed above. Suppose we calibrate on the call data and simply hold the parameters constant and apply them to pricing put options (representing our unknown option), this would mimic to some extent the concept of pricing different types of options. Figure 3.3 shows the results of such a test.

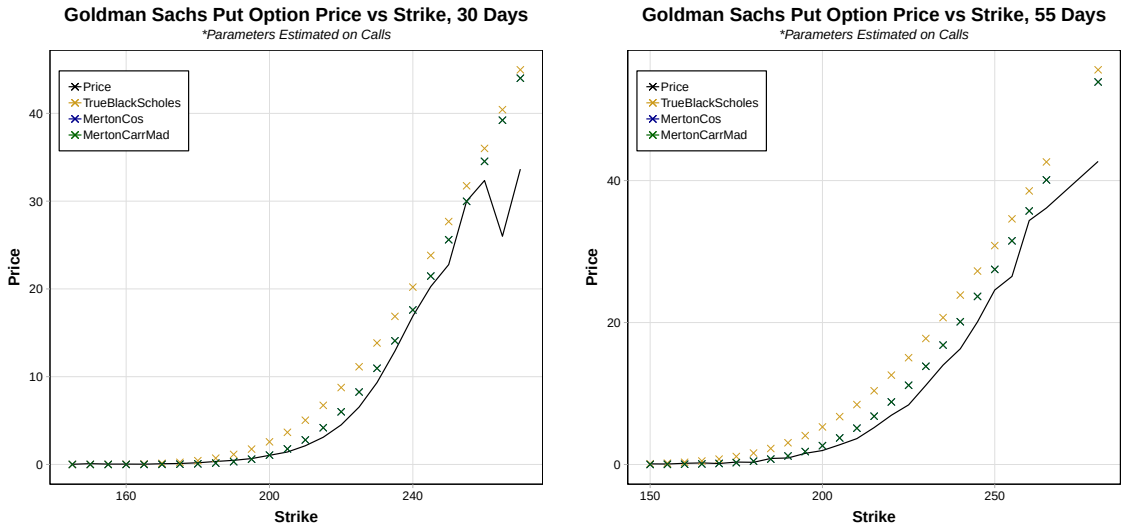

FIGURE 3.3: Post Calibration Put Prices at Various Times to Maturity with Parameters Estimated on Call Prices

Again we see both Carr-Madan and COS are overlaying one another whilst the Merton jump model offers a better fit to pricing a different type option with parameters calibrated from vanilla call data. We note that the call and put options are not ideal to test pricing new options given that there is likely a correlation between the two, however, the result is still important as it shows the robustness of the parameter estimation techniques and offers a visual interpretation of the modelling accuracy where it is unclear on how to obtain the precision of the calibration.

3.6 Volatility Smile

One of the shortcomings of vanilla Black-Scholes is its ability to capture the "volatility smile" phenomenon. Up until 1987 option prices as a function of strike and time-to-maturity resulted in a flat implied volatility surface (where implied volatility is the volatility observed when solving backwards for σ from market prices in Black-Scholes). Thus, if the real markets obeyed the Black-Scholes model, the implied volatility of all options written on the same underlying would be equal to the standard deviation of returns of this underlying [15]. In jump-diffusion models the implied volatility is both different from the historical volatility and changes as a function of strike and maturity offering an explanation of the implied volatility smile phenomenon. Due to data restrictions we are unable to replicate the smile as the market data contains observations that are unrealistic, this can also be seen by the figures shown in the model calibration section where there are various spikes in the market data price series.

It is unclear as to why the data displays this behaviour, however, we postulate that it may either be as a result of a calender effect (the TSLA 173 day data is very "jumpy") or a result of the trading volumes of the different options varying greatly as the data is not necessarily from a single index and source but rather compiled from Yahoo finance. Tankov and Voltchkova provide evidence that Lévy jump-diffusions capture the volatility smile.

Chapter 4

Risk Management under Levy Jump-Diffusions

The development of finance has led to an increase in the demand for managing the risk associated with asset management, as portfolio construction is largely affected by the risk-reward trade-offs we see in financial markets. Risks are broadly classified into three categories; business, strategic and financial risk [5]. Financial risk is associated with movements in the financial markets, in particular market risk - a subcategory within financial risk - is associated with changes in the prices of financial assets and liabilities.

Measuring risk plays a vital role in financial theory, up until now we have developed an option and equity share modelling framework under Lévy jump-diffusions, this framework allows us to examine the dynamics of portfolios comprised of both shares and options - so called non-linear portfolio's. As we are interested in the tail behaviour of portfolio's we will utilise a quantile based risk measure obtained from the distribution of returns to quantify the downside exposure to an asset. As the parameters of such a distribution are unknown and must be estimated from the data we should report precision estimates to account for the uncertainty attached to the risk measure calculated from the empirical data. For our purposes such precision will be reported in the form of confidence intervals. We also extend our models to a multivariate setting in order to study the tail dynamics of portfolios consisting of multiple shares.

4.1 Value-at-Risk

Value-at-Risk is considered an easy to understand risk measure making it conceptionally attractive, so much so that the Basle Committee permitted banks to calculate their capital requirements for market risks by means of VaR models [5]. For this reason we will consider only this risk measure in our thesis, however the results we derive can easily be extended to other quantile based risk measures such as Conditional Tail Expectation (CTE).

The VaR of a portfolio can be defined as the maximum expected loss that may be suffered on that portfolio over a specific time horizon (usually short-term), during which the composition of the portfolio remains unchanged [5]. VaR is subject to some confidence level, typically in the range of 95 to 99.9 per cent. Thus strictly speaking VaR attempts to answer the question, "What is the level of loss that we are x% confident shall not be exceeded in the short-term (N days)?" From this definition we can determine that VaR requires three components; an initial price, a time horizon and a confidence level. In a statistical sense, VaR is a percentile of the return distribution of the portfolio.

4.2 Tail Dynamics Of Non-Linear Portfolios

Portfolios consisting of only shares have a value function that is a linear combination of the assets on the market, however since options are non-linear functions of the values of their underlying assets, portfolios consisting of both shares and options are termed non-linear portfolios. As option contracts have non-linear pay-off functions the distribution of their values and of portfolios that contain them may be asymmetrical and exhibit unusual tail behaviour. This creates difficulties when modelling the returns of such portfolios with distribution functions. For this reason the traditional approach to computing risk measures such as VaR on these portfolios is by using Markov chain Monte carlo (MCMC) methods whereby observations of the portfolio returns are simulated and VaR is computed empirically from these observations.

Figure 4.1 illustrates the difficulty of fitting distributions to the returns of such portfolios. We simulated the value returns of a portfolio with 50% of its value in Tesla Shares and 50% of its value in Tesla Puts. Parameters were estimated using COS-MLE Estimation and the puts were priced according to the Merton model. The simulation period was 55 days and we assumed the puts were purchased at the beginning of the period at-the-money with 55 days till maturity. The simulation was run 300 times. In black we have a normal distribution fit to the simulated daily log returns and in red we have the infinitely divisible distribution corresponding to the Merton model. A close up on the left tail (b) reveals that both models are unable to properly capture the tail dynamics of the portfolio and VaR computed from these distributions would result in a misestimation.

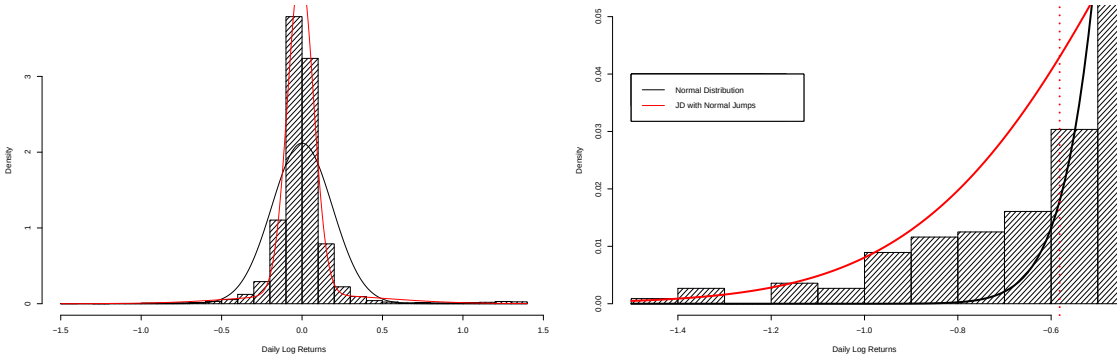

(a) Complete Histogram (b) Left Tail

FIGURE 4.1: Daily Log Returns of 50% Tesla Shares, 50% Tesla Puts portfolio

The problem with the traditional approach is that when MCMC methods are used share returns are often sampled from the normal distribution and option prices computed under the Black-Scholes framework. The result is that extreme movements in the share price are severely under represented in the simulated observations (as the tails of the normal distribution are thinner than those of the real returns). Building on results presented in Chapters 2 and 3, we propose an MCMC approach where returns are modelled using a Lévy jump-diffusion and option prices are computed under this same assumption.

4.2.1 Empirical Comparison, Traditional MCMC vs MCMC with Jumps

In order to empirically compare VaR estimation results obtained using the traditional approach MCMC against the proposed MCMC approach which allows for jumps in the asset prices we will consider the following one underlying asset dependent non-linear portfolios, comprised of Goldman Sachs (GS) shares and options:

	Assets		
	GS Shares	GS Puts	GS Calls
Portfolio 1	0.50	0.00	0.50
Portfolio 2	0.50	0.50	0.00
Portfolio 3	0.50	0.25	0.25

TABLE 4.1: Experiment Portfolio Weights

In our simulations we use a 30 day simulation period and assume that all options are bought at-the-money on the first day of the simulation period. For the traditional approach share returns will be sampled from the normal distribution and options priced according to the Black-Scholes Formula. For the MCMC with jumps log returns will be assumed to be Brownian motion with normal jumps and options will be priced according to the Merton model. Parameters for the simulation were estimated on historical data and the Merton model for option pricing was calibrated as in Chapter 3. Table 4.2 displays the estimated and calibrated parameter values used for the simulations.

	Parameters				
Instrument	μ	σ	λ	m	δ
(Merton) GS Shares	-0.0916	0.2850	1.4692	-0.0088	0.1062
(Merton) GS Options	—	0.2850	0.7075	0.0006	0.0002
(Black-Scholes) GS Shares	0.0099	0.3778	—	—	—
(Black-Scholes) GS Options	—	0.3778	—	—	—

TABLE 4.2: Simulation Parameters, $r = ln(1.02)$ and no dividend payouts.

Table 4.3 shows the results of the MCMC daily VaR estimation assuming 1 unit of currency was invested in the portfolio at the beginning of the simulation period. For all 3 portfolios the jump model produced more pessimistic estimates and wider confidence intervals than continuous model. Given that extreme events are under represented in the traditional MCMC, these results are as expected.

	Portfolio		
	1	2	3
Black-Scholes: $VaR_{95\%}$	0.1291	0.1105	0.0759
Merton: $VaR_{95\%}$	0.1882	0.1517	0.0939
Black-Scholes: $Conf_{95\%}(VaR_{95\%})$	[0.0566,0.2209]	[0.0652,0.1800]	[0.0262, 0.1335]
Merton: $Conf_{95\%}(VaR_{95\%})$	[0.0960, 0.2817]	[0.0760,0.2378]	[0.0429 ,0.1683]

TABLE 4.3: Single Asset MCMC VaR Results

4.3 Modelling Returns with Multi-dimensional Lévy Jump-Diffusions

In the case of linear portfolios, such as portfolios comprised of only shares it is much simpler and common practise to model share returns by fitting probability distributions to returns of the portfolio. The traditional approach assumes that the joint distribution of asset returns follows a multivariate normal distribution. The key advantages of this model is that the dependence structure between assets returns is completely specified by the covariances of the assets and that linear combinations of the margins of the multivariate normal are normally distributed with easily obtainable mean and variance parameters. These properties imply that the distributions of linear portfolios under this model are easily obtained and their parameters easily estimated. However, the problems introduced by the continuous sample paths of share prices implied by modelling log returns with a normal distribution extend to the multivariate setting. For this reason we attempt to relax this assumption in the multivariate case.

4.3.1 Constructing Multi-dimensional Lévy Models

There exist various methods in the literature for the construction of multi-dimensional Lévy models. A simple method is to time change multivariate Brownian motion. Such models are however limited in the type of dependence patterns they can describe (e.g. the cannot describe independence) [15]. Additionally the margins for such processes would be Lévy processes but not Lévy jump-diffusions and their margins must be the same process. For these reasons constructing multi-dimensional models in this manner is not appealing to us.

Definition of a Multi-Dimensional Lévy Jump-Diffusion

We define an $\mathbb{R}^d$-valued stochastic process $\boldsymbol{X}_t$ as a d-dimensional Lévy jump-diffusions if its margins $X_t^1, X_t^2, \cdots X_t^d$ are all Lévy jump-diffusions as defined in 2.1.2.

In-order to use such a process to model asset returns, we require a method of specifying the dependence structure of this process. One such method would be by using copulas, however the number of copulas required to fully describe the dependence structure does not scale well with the number of dimensions and this method is only feasible in low-dimension problems [15]. Kallsen and Tankov present an alternative method to describing the dependence structure using Lévy copulas (see [7] for a full description of this method) but unless the processes are restricted to make only positive jumps this method is complex.

To model the dependence structure of share returns we will construct a multi-dimensional Lévy jump-diffusion based on a two factor representation of the dynamics of asset returns. This method is presented in [1] where it is used to price products written on more than one underlying asset. The model is constructed from the fact that linear combinations of independent Lévy processes are also Lévy processes.

Let $Z_t, Y_t^j, j = 1, ..., n$ be independent Lévy processes on a probability space $(\Omega, \mathcal{F}, \mathbb{P})$ with characteristic functions $\phi_Z(u;t)$ and $\phi_{Yj}(u;t)$, for $j = 1, ..., n$ respectively. Then for $a_j \in$

$\mathbb{R}, j = 1, ..., n$

$$\boldsymbol{X}_t = \begin{bmatrix} X_t^1 \\ X_t^2 \\ \vdots \\ X_t^n \end{bmatrix} = \begin{bmatrix} Y_t^1 \\ Y_t^2 \\ \vdots \\ Y_t^n \end{bmatrix} + \begin{bmatrix} a_1 \\ a_2 \\ \vdots \\ a_n \end{bmatrix} Z_t \tag{4.1}$$

is a Lévy process on $\mathbb{R}^n$. The resulting characteristic function is

$$\phi_X(\boldsymbol{u}; t) = \phi_Z\left(\sum_{j=1}^{n} a_j u_j; t\right) \prod_{j=1}^{n} \phi_{Y^j}(u; t), \ \boldsymbol{u} \in \mathbb{R}^n \tag{4.2}$$

Additionally, by the properties of Lévy processes we have that for any $j \neq l$, the covariance between the j^{th} and l^{th} margin of $\boldsymbol{X}_t$ is

$$\text{Cov}(X_t^j, X_t^l) = a_j a_l \text{Var}(Z_1) t \tag{4.3}$$

The advantages of this modelling approach are that; simulation of the process extends easily from simulation of one dimensional Lévy jump-diffusions, a characteristic functions for the process and linear combinations of its margins are available, the parameter estimation methods presented in Chapter 3 can be extended for use in fitting this model. Additionally we can ascribe economic interpretations to the processes Z_t, Y_t^j, we will interpret Z_t as a model of the systemic risk that is common to all assets and Y_t^j as a model of the risk specific to asset j.

4.3.2 Fitting a d-Dimensional Lévy Jump-Diffusion

To fit the model given by Equation 4.1 to a given observed vector of returns we first select a proxy for the systemic component Z_t, usually some composite index. We fit a Lévy jump-diffusion and use equation 4.2 to obtain characteristic functions for the margins of $\boldsymbol{X}_t$. We use these characteristic function in conjunction with the parameter estimation procedures presented in Chapter 3 to estimate the parameters for the share specific Y_t^i components and the a_i parameters.

4.3.3 Results: A Comparison Against the Multivariate Normal

We fit a two dimensional model (for illustrative purposes) of the form given in 4.1 on the daily log returns of Bank of America (BAC) and Wells Fargo (WFC) two shares on the New York Stock Exchange (NYSE), while treating the NYA - a composite index of shares on the NYSE - as a proxy for the systemic process Z_t. We model this process with a Lévy Jump Diffusion with double exponential jumps. We model the share specific Y_t^j components with a Lévy jump-diffusion with normal jumps. We will compare the VaR estimates from the resulting model to those of the multivariate normal distribution fit on the same data. (See appendix B.1 for parameter estimates).

Figure 4.2 shows the margins of the multivariate normal model as well as the margins of the 2 factor multivariate Lévy jump-diffusion overlaid on the actual data. We note that the margins of the latter produce a visibly better fit and capture the tails more accurately than the former.

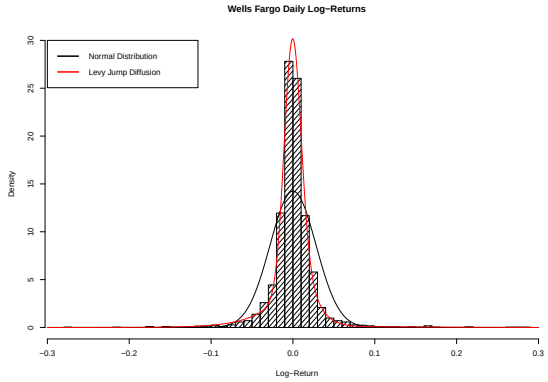

(a) BAC

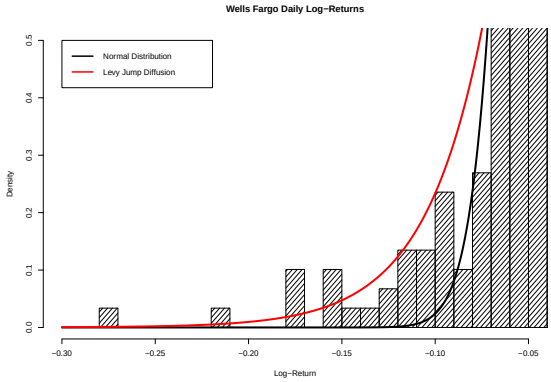

(b) BAC Lower Tail

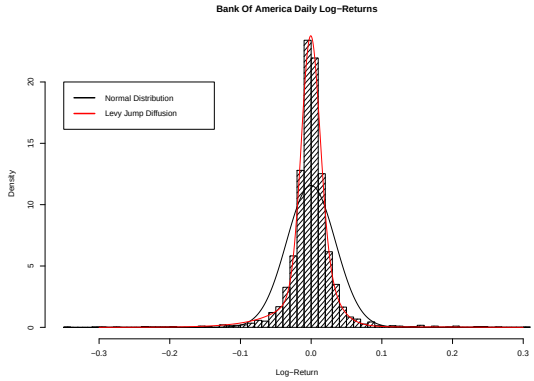

(c) WFC

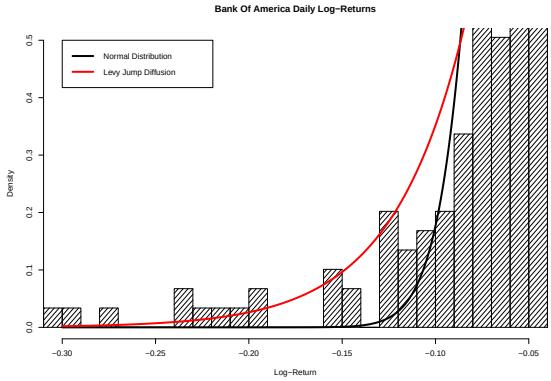

(d) WFC Lower Tail

FIGURE 4.2: Comparison of Margins

Let X_t^1 be the log return process of the BAC shares and X_t^2 be the log return process of the WFC shares. We consider a full invested, equally weighted portfolio consisting of these two shares. The return process of this portfolio R_t is thus given by:

$$R_t = \frac{1}{2}X_t^1 + \frac{1}{2}X_t^2.$$

Under the multivariate normal model R_t is normally distributed with easily obtainable mean and variance. Under the multivariate Lévy model we have fit, R_t has the following characteristic function:

$$\phi_{R_t}(u) = \phi_{X_t^1}\left(\frac{1}{2}u\right) \times \phi_{X_t^2}\left(\frac{1}{2}u\right),$$

Whose density can be recovered using the COS approximation detailed in Equation 2.13. Additionally its cumulative distribution function can be recovered by numerically computing;

$$\mathbb{P}[R_t \leq r] = \frac{1}{2} + \frac{1}{2\pi}\int_0^\infty \Re\left\{\frac{e^{iux}\phi_{R_t}(-u) - e^{-iux}\phi_{R_t}(u)}{iu}\right\}du. \tag{4.4}$$

The equation $\mathbb{P}[R_t \leq r] = \alpha$ can be solved numerically for r to obtain $(1-\alpha)\%$ VaR.

In order to report the uncertainty in our estimated parameters for the return distribution of the portfolio we perform a bootstrap with 100 bootstrap samples from the share return data. Computing a precision for VaR using bootstraps can be misleading due to the fact

that it is unlikely that the observations from which we draw our bootstrap samples are a complete representation of the true distribution of returns. This method is still preferable to alternatives such as extreme value theory based solutions which rely on asymptotic results since sufficient data is not always available and the convergence properties for such methods depend on the data and are thus difficult to predict.

For each bootstrap sample we estimate the parameters of our model and compute the 95% VaR giving us 100 estimates for VaR which we then use to obtain empirical confidence intervals. We compute VaR and its precision in this way under both the multivariate normal model and the multivariate Lévy model. We assume 1 unit of currency is invested in the portfolio.

	Multivariate Normal Model	Multivariate Lévy Model
$VaR_{95\%}$	0.0480	0.0377
$Conf_{95\%}(VaR_{95\%})$	[0.0442, 0.0525]	[0.0252 ,0.1082]

TABLE 4.4: Multi Asset Daily VaR Results

From the results illustrated in Table 4.4 we note that the multivariate Lévy model produces a less conservative VaR estimate than the multivariate normal model, however there is greater uncertainty around the estimation of this models parameters and this is reflected in the significantly wider VaR confidence intervals. It should be noted that parameters were estimated using the COS-MLE method with only 512 terms which could have increased the variation in the parameter estimates.

Chapter 5

Conclusion

Lévy jump-diffusions are the most mathematically tractable class of stochastic processes with discontinuous sample paths, as such they presented the an attractive method for modelling share prices whilst allowing for jumps. We found that such models produced better fits on empirical share returns and were able to more accurately capture option market price information than the geometric Brownian motion based Black-Scholes Model. Because these models more accurately represent the true return distribution they should in theory produce better VaR estimates than traditional methods. When considering non-linear portfolios we observed that the jump models produced more conservative estimates for VaR but in the multi-asset linear portfolio case neither the multivariate normal nor the 2 factor multivariate Lévy jump-diffusion produced consistently more or less conservative VaR estimates, though the former had significantly better precision.

The simplifying assumptions of stationary and independent increments mean that this class of models are still severely limited in their ability to account for some of the important empirical characteristics of real world share prices. Although the characteristic function of these processes is known in general, closed form expressions do no exists for the densities and must be recovered numerically. As a result usage of these processes is computationally involved and great care must be taken to balance the computational time and approximation errors in the parameter estimation, density recovery and calibration techniques. Obtaining better models for the dependence structure of multiple shares in the risk management application and applying change of measure theorems to obtain equivalent martingale processes in the option pricing application is non-trivial.

At the cost of further complexity better models can be obtained by relaxing the assumptions of stationary and independent increments allowing for the drift the diffusion components to be dependent on time and the value of the process. Such an approach is taken in [14], however their paper notes that the performance of such models were not significantly better than those we have presented.

Appendix A

R-Code

LISTING A.1: Simulates Sample Paths for Levy jump-diffusions

```
Sim.LevyJumpDiffusion <- function(b, c, lambda, N, Jump.Jen, ...)
{
  if(missing(Jump.Jen))
  {
    return(cumsum(c(0,rnorm(N,b,c))))
  }else{
    gen <- match.fun(Jump.Jen)
    Nt = rpois(1, lambda*N)
    U <- sort(runif(Nt,0,N))
    Y <- gen(Nt,...)
    times <- 1:N
    Cp <- vector("double", N)
    for ( i in 1:length(times))
    {
      Cp[i] <- sum(Y[U < times[i]])
    }
    brownianComponent <- cumsum(rnorm(N,b,c))
    return(c(0,brownianComponent + Cp))
  }
}
```

LISTING A.2: Estimate MLE Parameters for a Given Characteristic Function

```
CosEstimate <- function(Xi,  # data
                        carFun,  # Vectorized Characteristic
                           Function
                        theta,  # starting Parameter Vector for
                           carfun
                        a=-10, b=10,
                        N=10000,   # Number of expantion terms,
                           increase if obtaining
                        #errors
                        t=1/250, # time
                        ...  #  Additional parameters for optim
)
{
  k <- 1:(N-1)
  carFun <- match.fun(carFun)
  cos.p <- cos((k*pi/(b-a))%*%t(Xi-a))
  exp.p <- exp(-1i*k*a*pi/(b-a))
  arg.p <- k*pi/(b-a)
  X.p <- rbind(rep(0.5, length(cos.p[1,])), cos.p)
  objective <- function(par)
  {
```

```
    Fk <- function(k.in, theta){
      2/(b-a) * Re(carFun(k.in, theta,t)*exp.p)
    }
    Fk.o <- 2/(b-a) * Re(carFun(0, par,t))
    Fk.k <- c(Fk.o, Fk(arg.p, par))
    res <- sum(log(Fk.k %*% X.p))
    return(-res)
  }
  return(optim(theta, objective,...))
}
```

LISTING A.3: Estimate ECF Parameters for a Given Characteristic Function

```
ECFEstimate <- function(data,charFun,theta0, t =1/250, ...)
{
  charFun <- match.fun(charFun)
  h <- Vectorize(function(u,x, phi, theta,t)
  {
    phi <- match.fun(phi)
    out <- exp(-u^(2))*abs((1/length(x)*sum(exp(1i*u*x)) - phi(u,
       theta,t)))^2
    return(out)
  },"u")
  objective <- function(observations,phi,theta,t)
  {
    integrate(h,lower = -Inf, upper = Inf, x=observations,phi=phi,
       theta=theta,t=t)$value
  }
  nlm(objective, theta0, phi=charFun, observations=data, t=t, ...)
}
```

LISTING A.4: Recover Density Function from Characteristic Function

```
dchar.cos <- function(x, #  Data
                      CarFun,  # Vectorized Characteristic Function
                      theta,  # Parameter Vector for carfun
                      a=-5, b=5,
                      N=1000,  # Number of expantion terms,
                         increase if
                      #obtaining errors
                      num.cores = detectCores(), t = 1, ...)

{
  CarFun <- match.fun(CarFun)
  Fk <- function(k){
    2/(b-a) * Re (CarFun(k*pi/(b-a),theta,t,...)*exp(-1i*k*a*pi/(b-
       a)))
  }
  k <- seq(1,N-1)
  Fk.k <- vector("double", N-1)
  Fk.k <- unlist(mclapply(X=k,FUN=Fk, mc.cores = num.cores))
  Fk.o <- Fk(0)
  trans <- vector("double", N)
  trans <- unlist(mclapply(X=x, FUN=function(x) 0.5*Fk.o +
                             sum(Fk.k*cos(k*pi*(x-a)/(b-a))), mc.
                                cores = num.cores))
  return(trans)
}
```

LISTING A.5: Produce European Option Prices Using COS Method

```
COS.LevyOptionPrice.European <- function(
  So, # Share Price at t = 0
  K, # Strike Price
  t, # time till maturity
  carFun, # characteristic function of levy jump diffusion
  theta, # Parametet vector for levy jump diffusion
  r, # risk free interest rate
  call = T, # european call, if false returns put price
  q = 0,  # continous dividend yield
  N = 512,  # number of foureir cosine terms
  a = -10,  # lower trucation point
  b = 10,  # upper truncation point
  ...
)
{
  carFun <- match.fun(carFun)

  x <- log(So/K)

  chi_k  <- function(k, c, d)
  {
    1/(1 + (k*pi/(b-a))^2) * (cos(k*pi*(d-a)/(b-a))*exp(d) - cos(k*
       pi*(c-a)/(b-a))*exp(c)
                              + k*pi/(b-a)*sin(k*pi*(d-a)/(b-a))*
                                 exp(d)
                              - k*pi/(b-a)*sin(k*pi*(c-a)/(b-a))*
                                 exp(c))
  }

  phi_k <- Vectorize(function(k, c, d)
  {
    if(k==0)
    {
      res <- (d - c)
    }else{
      res <- (b-a)/(k*pi)*(sin(k*pi*(d-a)/(b-a)) - sin(k*pi*(c-a)/(
         b-a)))
    }
    return(res)
  }, "k")

  k <- seq(1, N-1)

  Uk <- 2/(b-a) * (-chi_k(k,a,0) + phi_k(k,a,0))
  Uk.o <-2/(b-a) * (-chi_k(0,a,0) + phi_k(0,a,0))

  exp.p <- matrix(unlist(lapply(x, function(x) exp(1i*k*pi*(x-a)/(b
     -a)))),
                  length(k),length(x))

  terms <- (carFun(k*pi/(b-a), theta=theta, t=t, r=r, d=q,...) * Uk
     ) %*% exp.p


  val <- K*exp(-r*t)*Re(0.5*Uk.o + colSums(terms))
  if(call) val <- So - K*exp(-r*t) + val  # Put Call Parity
```

```
  return(val)
}
```

LISTING A.6: Produce European Option Prices Using Carr-Madan Method

```
CarMadanOptionPrice <- function(So, # Share Price at t = 0
                                K, # Strike Price
                                t, # time till maturity
                                carFun, # characteristic function
                                   of levy jump diffusion
                                theta, # Parametet vector for levy
                                   jump diffusion
                                r, # risk free interest rate
                                call = T, # european call, if false
                                    returns put price
                                d = 0,  # continous dividend yield
                                alpha = 1,
                                ...

)
{

  carFun2 <- function(v, theta, t, delta, ...){
    exp(1i * v * log(So)) * match.fun(carFun)(v, theta, t, delta,
       ...)
  }

  Car_Madan <- Vectorize(function(K){

    fx <- Vectorize(function(v)
    {
      Re( exp(-1i*v*log(K))*( (exp(-r*t) * carFun2((v-(alpha + 1)*1
         i),
                                                   theta, t, r - d
                                                      ,...)) / (
                                                      alpha^2 +
                                                      alpha - v^2 +
                                                       1i*(2*alpha
                                                      + 1)*v)) )
    }, "v")

    exp(-alpha*log(K))/pi * as.numeric(integrate(f = fx, lower = 0,
        upper = Inf)[1])

  }, "K")

  price <- rep(0, length(K))
  if(call == TRUE){
    price <- Car_Madan(K)
  }else{price <- Car_Madan(K) - So + K*exp(-r*t)}

  return(price)
}
```

LISTING A.7: Calculate Log Returns

```
returns.na <- function(St,period=1) (na.omit(diff(log(St),lag=
   period)))
```

LISTING A.8: Generate Observations from a Stable Distribution

```
rstable <- function(n, alpha=2, beta=0, gamma=1, delta=0)
{# Simulates S(a,b,g,d,1)
  U <- runif(n, -pi/2, pi/2)
  W <- rexp(n)
  C <- -beta*tan(pi*alpha/2)
  if(alpha!=1)
  {
    E <- 1/alpha * atan(-C)
    a.UE <- alpha*(U+E)
    X <- (1+C^2)^(1/(2*alpha)) * sin(a.UE)/((cos(U))^(1/alpha)) *
      (cos(U-a.UE)/W)^((1-alpha)/alpha)
    Y <- gamma*X + delta
  }else{
    E <- pi/2
    p.BU <- (pi/2 + beta*U)
    X <- 1/E * (p.BU*tan(U)-beta*log(0.5*pi*W*cos(U)/p.BU))
    Y <- gamma*X + 2/pi * beta*gamma*log(gamma) + delta
  }
  return(Y)
}
```

LISTING A.9: Compute Black Scholes Option Prices

```
bs.Price <- function(So, K, r, sigma, call = T, t)
{
  d1 <- 1/(sigma*sqrt(t)) * (log(So/K) + (r + sigma^2/2)*(t))
  d2 <- d1 - sigma*sqrt(t)
  C <- function(s,t) pnorm(d1)*(s) - pnorm(d2)*K*exp(-r*t)
  if(call)
  {
    res <-  C(So,t)
  }else{
    res <- K*exp(-r*t) - So + C(So,t)
  }
  return(res)
}
```

LISTING A.10: Converts Characteristic Function to Distribution Function

```
pchar <- Vectorize(function(x, phi, theta, lower.tail=T,t=1/250)
{ # Takes in charecteristic function returns cdf
  phi <- match.fun(phi)
  integrand <- function(u,x)
  {
    Re((exp(1i*u*x)*phi(-u,theta,t) - exp(-1i*u*x)*phi(u,theta,t))/
       (1i*u))
  }
  val <- 0.5 + 1/(2*pi) * integrate(integrand, lower = 0, upper =
     Inf, x=x)$val
  if(!lower.tail) val <- 1 - val
  return(val)
},"x")
```

LISTING A.11: Converts Characteristic Function to Quantile Function

```
qchar <- Vectorize(function(p, phi, theta, lower.tail=T,t=1/250)
{ # Takes in charecteristic function returns quantile function
```

```
  if (!lower.tail) p <- 1-p
  val <- uniroot(function(x) pchar(x, phi, theta,t=t)-p, c(-1,0))$
     root
},"p")
```

LISTING A.12: Generates Observations from the Double Exponential Distribution

```
rdoubleexp <- function(n, p=0.5, eta1=1, eta2=1)
{ # simulate from kous double exponential distribution
  s <- rbinom(n,1,p)
  val <- vector("numeric", n)
  val[s==T] <- rexp(sum(s==T),rate=eta1)
  val[s==F] <- -rexp(sum(s==F),rate=eta2)
  return(val)
}
```

LISTING A.13: Objective for Model Calibration

```
# COS Objective function
objective.cos <- function(theta)
{
  Pobs <- Price  # Real Prices
  wi <- (1/Pobs)^2  # weight vector
  Pmodel <- COS.LevyOptionPrice.European(So, Strike,
                                         t, char.fun.mertonprice,
                                            theta, r,
                                         N = 1024, sigma)
  sum(wi*(Pobs - Pmodel)^2)
}

# Carr Objective function
objective.car <- function(theta)
{
  Pobs <- TSLA2018_new_5day_call$Price  # Real Prices
  wi <- (1/Pobs)^2  # weight vector
  Pmodel <- CarMadanOptionPrice(So, Strike,
                                t, char.fun.mertonprice, theta, r,
                                sigma)
  sum(wi*(Pobs - Pmodel)^2)
}
```

Appendix B

Parameter Estimates

B.1 4.3.3

Table showing parameter estimates used in section 4.3.3. Parameters Estimated using COS-MLE with share price data from 2007-01-04 to 2018-10-18.

	Parameters								
Component	μ	σ	λ	m	δ	λ_1	λ_2	p	a_i
BAC: Y_t^1	-0.5237	0.0622	1.1917	0.1691	0.0521	—	—	—	2.1022
WFC: Y_t^2	-0.3597	0.0206	2.4377	-2.1170	0.0626	—	—	—	1.7055
NYA: Z_t	0.0341	0.0911	154.79	—	—	151.79	59.882	0.6752	—

TABLE B.1: Parameter Estimates for Comparison in 4.3.3

Bibliography

[1] Ballotta, Laura and Bonfiglioli, Efrem. "Multivariate asset models using Lévy processes and applications". In: *The European Journal of Finance* 22.13 (2016), pp. 1320–1350.

[2] Black, Fischer and Scholes, Myron. "The Pricing of Options and Corporate Liabilities". In: *Journal of the Political Economy* (1973).

[3] Carr, Peter and Madan, Dilip. "Option valuation using the fast Fourier transform". In: (1999).

[4] Fang, Fang and Oosterlee, Cornelis W. "A novel pricing method for European options based on Fourier-cosine series expansions". In: *SIAM Journal on Scientific Computing* 31.2 (2008), pp. 826–848.

[5] Goorbergh, Rob WJ van den, Vlaar, Peter JG, et al. *Value-at-Risk analysis of stock returns historical simulation, variance techniques or tail index estimation?* De Nederlandsche Bank NV, 1999.

[6] Iacus, Stefano M. *Option pricing and estimation of financial models with R*. John Wiley & Sons, 2011.

[7] Kallsen, Jan and Tankov, Peter. "Characterization of dependence of multidimensional Lévy processes using Lévy copulas". In: *Journal of Multivariate Analysis* 97.7 (2006), pp. 1551–1572.

[8] Kou, Steven G. "A Jump-Diffusion Model for Option Pricing". In: *Management Science* (2002).

[9] Merton, Robert C. "Option Prices When Underlying Stock Returns Are Discontinuous". In: *Journal of Financial Economics* (1976).

[10] Papapantoleon, Antonis. "An Introduction to Lévy processes with applications in finance". In: *arXiv preprint arXiv:0804.0482* (2008).

[11] R Core Team. *R: A Language and Environment for Statistical Computing*. R Foundation for Statistical Computing. Vienna, Austria, 2018. URL: https://www.R-project.org/.

[12] Ryan, Jeffrey A. and Ulrich, Joshua M. *quantmod: Quantitative Financial Modelling Framework*. R package version 0.4-13. 2018. URL: https://CRAN.R-project.org/package=quantmod.

[13] Sato, Ken-iti and Ken-Iti, Sato. *Lévy processes and infinitely divisible distributions*. Cambridge university press, 1999.

[14] Sepp, Artur. "Pricing european-style options under jump diffusion processes with stochastic volatility: Applications of fourier transform". In: (2003).

[15] Tankov, Peter and Voltchkova, Ekaterina. "Jump-diffusion models: a practitioner's guide". In: *Banque et Marchés* 99.1 (2009), p. 24.

[16] Yu, Jun. "Empirical characteristic function estimation and its applications". In: *Econometric reviews* 23.2 (2004), pp. 93–123.